European
Commission

JRC TECHNICAL REPORTS

# Field guide for forest mapping with high resolution satellite data

*Monitoring deforestation and forest degradation in the context of the UN-REDD programme*

*The Tanzania REDD+ initiative*

Lorena Hojas Gascón and Hugh Eva

2014

Report EUR26922 EN

Joint
Research
Centre

European Commission
Joint Research Centre
Environment and Sustainability

Contact information
Hugh Eva
Address: Joint Research Centre, Via Enrico Fermi 2749, TP 260, 21027 Ispra (VA), Italy
E-mail: hugh.eva@jrc.ec.europa.eu
Tel.: +39 0332 78 5016

http://ies.jrc.ec.europa.eu/
http://www.jrc.ec.europa.eu/

This publication is a Technical Report by the Joint Research Centre of the European Commission.



JRC92600

EUR 26922 EN

ISBN 978-92-79-44012-0 (PDF)

ISSN 1831-9424 (online)

doi:10.2788/657954

Luxembourg: Publications Office of the European Union, 2014

# Contents

## List of Tables

## List of Figures

## Abbreviations

CBD……………………………………………………………………………………………….Convention on Biological Diversity
COP………………………………………………………………………………………………………………..Conference of the Parties
DBH…………………………………………………………………………………………………………….Diameter at Breast Height
DG DEVCO…………………Directorate General for Development and Cooperation of the European Union
FAO……………………………………………………………………….United Nations Food and Agriculture Organization
GIS…………………………………………………………………………………………………Geographic Information Systems
GPS……………………………………………………………………………………………………………..Global Positioning System
IPCC……………………………………………………………………………….Intergovernmental Panel on Climate Change
ITTO……………………………………………………………………………….International Tropical Timber Organization
IUFRO………………………………………………………………International Union of Forest Research Organizations
JRC……………………………………………………………………………………………………………… Joint Research Centre
NAFORMA……………………………………………………….National Forest Monitoring and Assessment program
MMU…………………………………………………………………………………………………………..Minimum Mapping Unit
MNRT……………………………………………………………Ministry of Natural Resources and Tourism of Tanzania
TFS…………………………………………………………………………………………………………….Tanzania Forest Service
TREES-3………………………………………………………………….Tropical Environmental Monitoring by Satellite
ReCaREDD……………………………………………………………………………………………...Regional Capacities for REDD
REDD……………………………………………………………Reducing Emissions from Deforestation and Degradation
UNFCCC………………………………………………….. United Nations Framework Convention on Climate Change
UTM………………………………………………………………………………………………………Universal Transverse Mercator

## Background

An important part of remote sensing science is the calibration and validation of maps and products derived from satellite images using 'ground truth', that is, *in situ* measurements. For statistical assessments, large quantities of reference points are required. Extensive field data are difficult to obtain for reasons of access, manpower, timing and costs and usually can only be undertaken by national forest agencies. These latter data are not always available to outside institutions and may not always target the application envisaged by other users.

This manual is targeted at guiding the collection of adequate field information in a relatively short time, for calibrating and validating classifications and biophysical parameters derived from satellite images of high spatial resolution for forest monitoring. These products have been shown to be useful to increase the effectiveness of suitable forest management at local level, e.g. to control the fuel wood production capacity and detect areas of illegal harvesting. In the future, they will allow us to improve the assessment of forest biomass and carbon budgets changes at national level, with the aim of monitoring deforestation and forest degradation in the context of the UN-REDD (Reducing Emissions from Deforestation and Degradation) programme.

The area of study is Tanzania, one of a number of pilot countries which has received direct support by the UN to carry out a national REDD+ initiative. Field survey was carried out in conjunction with the Tanzania Forest Service in 2012, 2013 and 2014. The field data collected in this work were used to produce maps of forest cover, basal area and biomass. These maps were transferred to the Tanzania Forest Service.

The field survey was executed using basic, readily available and inexpensive methods (standard GPS, digital camera and paper data forms) so as to ensure that all services can carry out a similar exercise. More sophisticated equipment combining GPS, camera, data logger and GIS are available, but remain relatively expensive. As such equipment become available at lower prices, it will become feasible to collect more data in less time.

## Acknowledgements

Without the cooperation of the Tanzania Forest Services (TFS) and the Food and Agriculture Organization (FAO) of the United Nations the collection of the field data would not have been possible. The EU Delegation in Dar es Salaam was key to our efforts in effecting a collaboration agreement with the Tanzanian authorities. Support to this technical report was provided by the ReCaREDD project (Regional Capacities for REDD+) funded by services of the European Commission (DG DEVCO). In particular the field mission conducted in Tanzania in June 2014 was funded under ReCaREDD. Ms. Hojas was funded by a JRC doctoral grant hosted by the University of Valencia, and subsequently sponsored by CIFOR, the Center for International Forestry Research - Bogor, under a Collaboration Agreement with the JRC. The UN-REDD Tanzania provided research the permits required to carry out work in the country. Finally, the authors wish to thank colleagues in their respective services and the JRC mission office for supporting our mission administration.

The authors would specifically like to thank the following for their support:

**The Tanzania Forest Service**
Mr. Juma Mgoo, Chief Executive Officer
Mr. Nurdin Chamuya
Dr. Rogers Malingwi
Dr. Jared Otieno
Dr. Boniface Mbilinyi
Mr. Mathew Mwamuo
Mr. Jonathan Tangwa
Mr. Robert Nyali
Mr. Iddy Beya
Mr. Ally J. Mtosa
Mr. Yoab Kusimula
Mr. Moses Tenisula
Mr. Msalika Pastory

**FAO**
Mr. Søren Dalsgaard, Chief Technical Advisor Tanzania
Mr. Mikko Leppänen, FIN-FAO
Dr. Anssi Pekkarinen, FIN-FAO
Mr. Lauri Tamminen, FIN-FAO
Mr. Amana, FAO
Mr. Philipe Crete, FAO-REDD

**FAO Representation in Tanzania**
Diane Tempelman, FAO representative in Tanzania

**EU Delegation in Tanzania**
Mr. Filiberto Ceriani Sebregondi, Head of Delegation in Tanzania
Mr. Gianluca Azzoni, Head of Natural Resources Section
Ms. Maria Iarrera

**University of Valencia**
Dr. Javier García Haro

**CIFOR**
Dr. Robert Nasi
Dr. Paolo Cerutti

This page is blank

# 1. Introduction

## 1.1 Monitoring deforestation in the tropics

For more than a decade the monitoring of deforestation has successfully been carried out at regional and national levels using moderate spatial resolution satellite data, predominantly from the 30 m spatial resolution Landsat sensor.

The Joint Research Centre (JRC) of the European Commission, under its TREES-3 project, has carried out forest cover change assessment in the tropics for the periods 1990-2000, 2000-2005 and 2005-2010 using a systematic sampling of Landsat image subsets. The sampling units of 20 km x 20 km are centred at the confluence of the geographical latitude and longitude integer degrees and cover the full tropical forest belt. They are classified at a minimum mapping unit of 5 ha in four main classes: tree cover (more than 70% of forest cover), tree cover mosaic (between 40 and 70% of forest cover), woody vegetation (shrubs and forest regrowth) and other land cover (Achard *et al*. 2009).

Similar projects have been carried out at national and regional scales, reaching accuracies of *ca.* 90% with different minimum mapping units up to 5 ha using Landsat data. The Brazilian National Space Agency (INPE) has carried out an annual wall-to-wall forest mapping of the Amazon based on remote sensing since 1989 (INPE 2014). The Food and Agricultural Organization (FAO) of the United Nations carried out a remote sensing exercise for supporting its five year global Forest Resource Assessment (FRA) survey based on country reports from the national forest services. The most recent FRA survey of 2010 was executed in the tropics by the Joint Research Centre (FAO, JRC, SDSU and UCL 2009). More recently the University of Maryland, in conjunction with Google, have produced global forest change maps based on a synthesis of the Landsat archive for the years 2000-2012 (Hansen *et al*. 2013).

## 1.2 Monitoring deforestation and forest degradation for REDD+

REDD+ [1] activities proposed at the United Nations Framework Convention on Climate Change COP-16 (UNFCCC 2011), brought new requirements for monitoring deforestation, and also forest degradation, at national levels and at finer scales. At the UNFCCC COP-7 deforestation had been defined as a 'measurable decrease in tree crown cover below 10-30% of forest areas with a minimum size of 0.05-1 ha' (UNFCCC 2001). This is difficult to detect with high accuracy from the medium (c. 30 m) spatial resolution satellite data. Degradation, defined by default as a 'loss of carbon stock with a decrease in the tree crown cover not below the 10-30% threshold' at the UNFCCC COP-9 (IPCC 2003), is even more of a challenge to measure. Apart from these general definitions, each country can adopt its own definition of forest area, with the minimum mapping unit, tree crown cover and tree height, inside the thresholds provided by the UNFCCC.

The UNFCCC stated, and guided methodologically, that REDD+ should be implemented by *'establishing monitoring systems that use an appropriate combination of remote sensing and ground-based forest carbon inventory approaches, with a focus on estimating forest area changes, forest carbon stocks and anthropogenic forest-related greenhouse gas emissions by sources and removals by sinks'* (UNFCCC 2009). The addition of forest degradation in the program implies that

[1] Reducing emissions from deforestation and forest degradation in developing countries; and the role of conservation, sustainable management of forests and enhancement of forest carbon stocks in developing countries.

the estimations of forest carbon stock changes need to be based, not only on monitoring transitions of land cover classes (*e.g.* forest into non forest), but also on transitions within a class (*e.g.* forest into forest) when there is a loss of carbon sequestration. Again, every country can define its own definitions and methods (*e.g.* sampling design, carbon estimation approach, remote sensing techniques...) according to its policy goals, available data, affordable methods and particular vegetation characteristics.

The JRC through funding from DG DEVCO, has embarked on a research program called ReCaREDD, which combines a capacity building element, to develop remote sensing techniques to detect and eventually quantify forest degradation using finer spatial resolution satellite data in test sites across the tropics. Partnerships are being set up with a number of countries to test and implement methodologies. Tanzania is one such country, where in 2012 the JRC signed a Collaboration Agreement with the Tanzania Forest Services from the Ministry of Natural Resources to work jointly on this topic (EU 2013).

### 1.3 The Tanzania REDD+ initiative

Tanzania is one of the sixteen pilot countries which have received direct support by the UN to carry out a national REDD+ initiative (UN-REDD 2009). The National Forest Monitoring and Assessment program (NAFORMA), set up by the Ministry of Natural Resources of Tanzania (MNRT) and UN-REDD, with the technical support of FAO-Finland (UN-REDD 2012a), produced a national forest inventory, combining field survey with medium resolution satellite data (NAFORMA 2010a). It aimed to become the national framework for assessing and monitoring forest carbon pools compatible with REDD+ requirements (UN-REDD 2012b).

The NAFORMA inventory employed a stratified sampling based on biomass density (predicted growing stock) and work efficiency (distance and time planning according to roads, foot paths and topography), which resulted in 32,660 field plots of 15 m radius across the country (Tomppo *et al.* 2010). From each plot data on canopy cover, tree height, trunk diameter, species, dead wood and soil were collected (NAFORMA 2010a). Using the field information a wall-to-wall land cover map of 2010 from Landsat data was also produced. Around 25% of the plots were selected as 'permanent plots' and are planned to be re-measured in the future every five years.

The forest definition adopted by NAFORMA and the Tanzanian national REDD+ strategy was an *'area of land with at least 0.5 hectares with a minimum tree crown cover of 10%* [2]*, and with trees which have the potential or have reached a minimum height of 5 metres at maturity in situ'* (UN-REDD, 2013). According to this definition, the spatial resolution of the Landsat sensor, while adequate for monitoring clear-cutting, is too coarse for monitoring deforestation and especially forest degradation (*i.e.* it should detect losses of carbon in tree covered areas less than a Landsat pixel). The JRC is supporting NAFORMA in developing methods to detect (map) and quantify forest degradation using higher spatial resolution satellite data (*i.e.* ≤ 10m).

### 1.4 The JRC approach for monitoring forest degradation in Tanzania

RapidEye satellite data of 5 m spatial resolution, corresponding to the 76 sample sites of the TREES-3 project which cover Tanzania, were acquired for the year 2010 (Figure 1, top image). In the scope of

[2] or with existing tree species, planted or natural, having the potential of attaining more than 10% of crown cover

the collaboration between the Tanzania Forest Service (TFS) and JRC, the goal was to process these satellites images to derive forest maps with thematic and quantitative classes; the transitions of these classes must be related to forest degradation processes (and severity) according to REDD+ specifications. Of course, degradation implies a change over time, and historical data of finer resolution are often not available.

To obtain these maps, firstly the images were divided into land units using image segmentation, classified in vegetation types, and remote sensing parameters were extracted from the forest units. Secondly, the best correlations between these parameters and field measurements related to forest degradation processes were identified. Finally, these correlations were used to classify the full image set. While the field data from NAFORMA may serve as a validation data set for the forest maps, sample sites are too few within individual RapidEye images to provide a calibration data set. To supplement these data, very high spatial resolution (≤ 1 m) satellite images from several satellites were foreseen as surrogate ground data for 14 sites distributed across the country in different ecosystems.

As a first step we carried out methodological tests on a limited number of sample sites for which we have very high resolution images. For each of these sites we have therefore data from Landsat, RapidEye and a very high spatial resolution satellite (Quickbird, Worldview-2 satellites, IKONOS or Geoeye-1) for the year 2010.

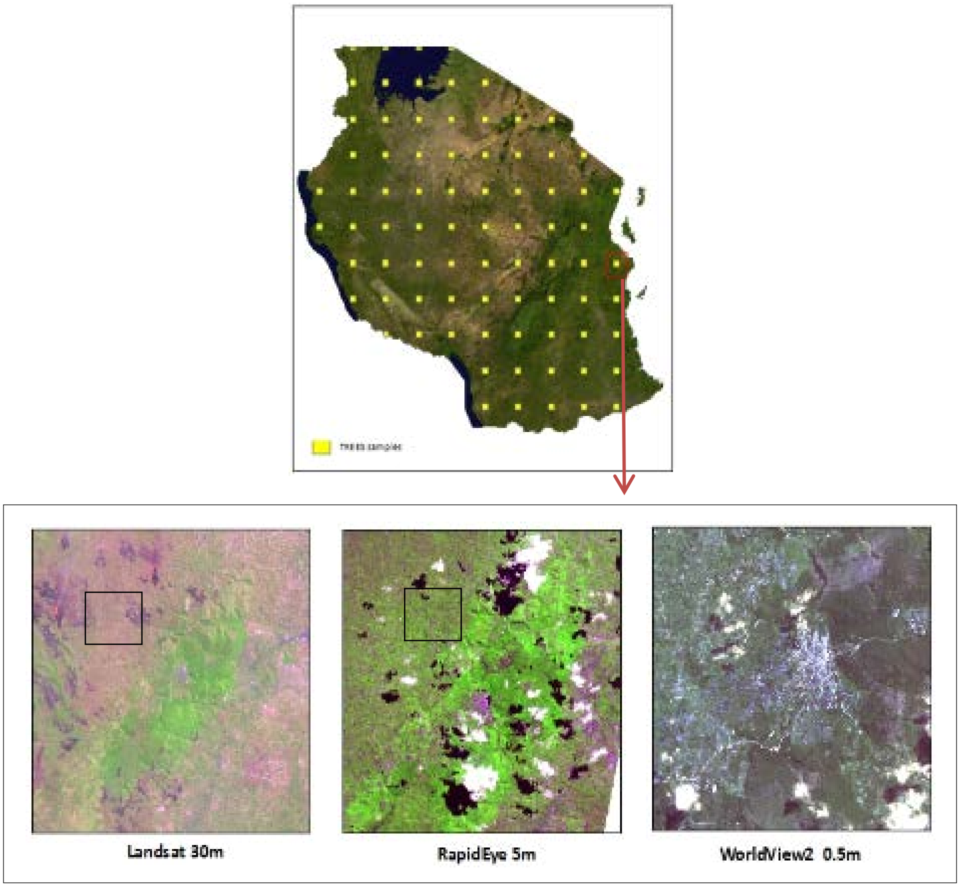


Figure 1: Location of the sample sites of the project (top image) covered by RapidEye data over a true colour mosaic of Tanzania from the MODIS sensor. Examples of Landsat, RapidEye and WordView-2 image subsets, 30 m, 5 m and 0.5 m spatial resolution respectively (bottom image), corresponding to the sample centred at 7°S 39°E coordinates (surrounded by a red square). The Wordview-2 image only covers a 7 km x 7 km subset of the sample site (square on the Landsat and Rapideye images).

## 1.5 Introduction and objectives of the field survey

Four short field missions were carried out in Tanzania during 2011, 2012, 2013 and 2014. In 2011 the Collaboration Agreement was established with the TFS and prospective pilot study sites were identified for the development of the methodology. In 2012 field work was carried out across different ecosystems in Tanzania to gain information on the vegetation types and the characteristics of forest degradation in different stages. There was a time restriction of two weeks for the field visits, which determined the number and extent of the sample sites. In 2013 the results were presented at the *'Workshop on the findings of the National Forest Monitoring and Assessment (NAFORMA)'* at the National Carbon Monitoring Centre in Morogoro (10-14$^{th}$ June 2013). A further field survey was carried out in 2014 to provide validation data for one of the sites.

The final objective of the field survey was to assemble a data set to calibrate the very high resolution satellite images for vegetation classification, and within the forest areas, discriminate degradation levels across the country. Therefore, the sampling method aimed to characterise the main forest types and conditions (canopy cover, carbon stock...) that could be identified on the satellite images, and not to support statistical national studies and long-term monitoring systems (as the intensive and repetitive stratified sampling from NAFORMA). The design of the field protocol (type of plots, measurements…) took into account the integration of the data with the NAFORMA field survey, so as to increase the number of samples per image.

## 1.6 Scope of the technical report

This technical report is aimed at supporting those carrying out field missions for land cover monitoring studies implemented with remote sensing data, rather than full ground inventories. Many countries lack extensive field survey data, and where they do exist, they are not always publicly available to external bodies. The scope of this report is therefore to provide guidance in planning, executing and exploiting a rapid field survey which can serve in the interpretation and validation of remote sensing data.

Field survey involves a heavy investment in time and funds, and to be useful for statistically valid studies needs to cover a significant number of sites. As it is not always possible to carry out long-term missions, we aimed at a field survey of 2 weeks duration. Such a survey therefore needs to be efficiently organized so as to obtain a representative number of samples. In this manual we focus on the thematic of forest monitoring, more specifically on degradation processes, however, the main concepts elaborated here can be applied to other areas of application (land cover changes, agricultural census etc.).

Throughout the report we use examples from our experience in the planning, execution and exploitation of data of our field missions in Tanzania. These three aspects include mainly:

1) Mission preparation: assembly of input data sets, selection of sample locations, design of field survey (measurements, sampling method, plot technique), elaboration of field documents and planning of logistic and legal matters. → *Sections 2 and 3*.
2) Mission implementation: design of a field measurement protocol, preparation of equipment and software and recording of data. → *Section 4.*
3) Data processing: data synthesis, data analysis and map production. → *Sections 5 and 6.*

# 2. Selection of field sites

The final goal of the field survey was to calibrate satellite images for vegetation classification, and within forest areas, discriminate degradation levels. Therefore, two objectives were set out for the choice of the location of the field sites:

1. To obtain an overview of the different types of vegetation formations and degradation processes existing in Tanzania. For this, we required a set of ***general field sites*** where rapid visits (with limited field work) were done, so as to gain first-hand experience of forest types and degradation dynamics throughout the country.
2. To get detailed information of one of the forest types in Tanzania. From the general sites, one was selected as the ***primary field site*** where intensive field work was carry out, in order to develop remote sensing methods for forest degradation monitoring.

## 2.1 General field sites

Our goal was to locate a maximum of four representative sites of the main ecoregions of the country. We wanted the sites to be located in areas i) with evidence of forest degradation processes, ii) where we could obtain supporting spatial and remote sensing data, and iii) with feasible accessibility. To determine the potential sites which complied with these characteristics, we assembled a geographic database of the country, reviewed the historical changes in forest areas, assessed the availability of satellite data and checked the accessibility through paths and roads.

### 2.1.1 Geodatabase compilation

We assembled a geodatabase of Tanzania to support the selection of the sites and the planning of the field visits. It included information about vegetation types, forest area changes, administrative units, climate, level of protection and land cover. Table 1 contains the list of the main data included in the geodatabase.

Table 1: Spatial data in the Tanzania geodatabase grouped by thematic.

| Thematic | Spatial data |
|---|---|
| Vegetation | White's vegetation map of Africa |
| | Global ecological zones of the World (FAO 2001) |
| | Huntings vegetation map of Tanzania |
| Forest changes | TREES deforestation and forest fragmentation statistics for the periods 1990-2000 and 2000-2010 |
| Administration, population and infrastructure | Regions and districts of Tanzania |
| | Cities and villages of Tanzania |
| | Roads of Tanzania |
| Climate | FAO climate classification according to elevation and rainfall |
| Protected areas | IUCN protected areas of Africa (national parks, national reserves, game reserves, World Heritage Convention areas) |
| | National protected areas of Africa (state and district protected forests) |
| Land cover | Global land cover for 2000 (GLC2000) |

#### 2.1.1.1 *TREES-3 forest statistics*

The TREES-3 study on measuring deforestation in the tropics (1990-2000-2010) has a statistical sampling designed for estimation of forest changes (deforestation, fragmentation, loss of tree cover and loss of woody vegetation) at continental level (Achard *et al*. 2014). It is not robust enough to make quantitative national estimates, unless the sampling is intensified (Eva et al. 2010); however, it can give us an indication of the forest dynamics going on in Tanzania related to loss of carbon stock in forest and woody vegetation areas.

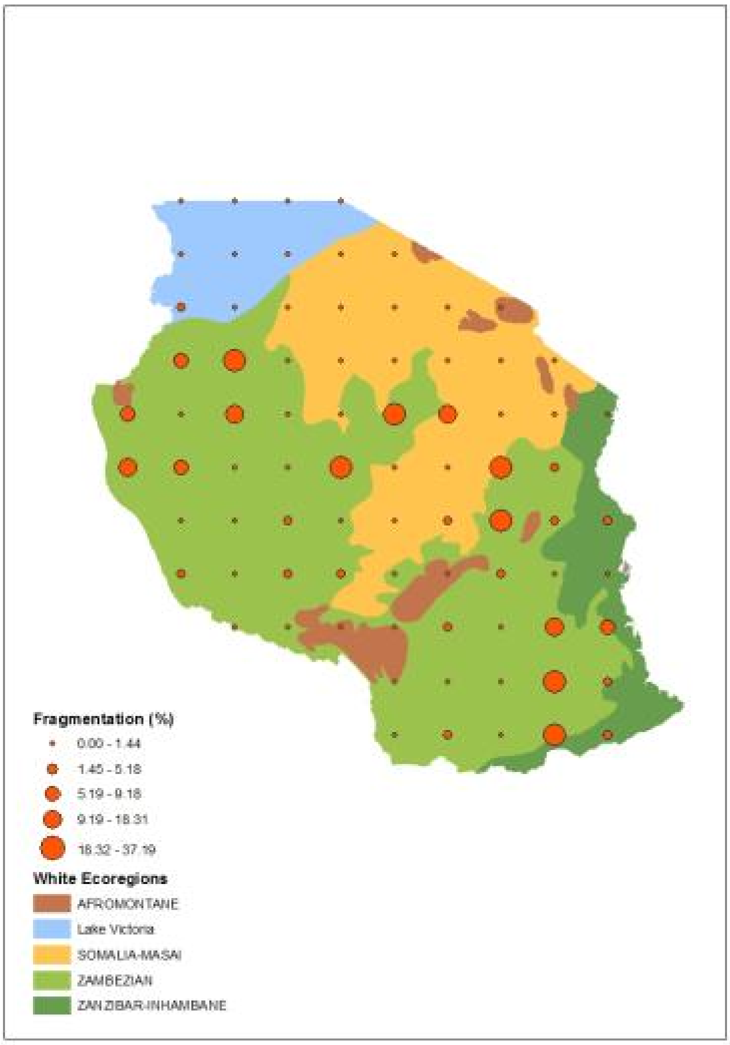


In Tanzania between 1990 and 2000 the main pattern of tree cover loss was forest fragmentation, this is, the conversion of tree cover into tree cover mosaic. In practical terms this means that forest areas of a minimum size of 5 ha with more than 70% of tree cover have been converted to areas with 40-70% of tree cover. Figure 2 depicts the percentages of forest fragmented area in the TREES sites over the White vegetation map.

In Tanzania, the Zambezian ecoregion, where woodland is the predominant and characteristic vegetation type, is the most affected by forest fragmentation, followed by the Zanzibar-Inhambane ecoregion. Together with forest fragmentation, loss of woody vegetation was the major change during the decade.

Figure 2: TREES-3 estimation of forest fragmentation from 1990 to 2000 overlaid on the White vegetation map. The size of the circles represents the percentage of tree cover area converted into tree mosaic.

### 2.1.2 Satellite image screening

Satellite images of very high spatial resolution were sought for those TREES-3 sample sites with evidence of forest degradation. Such information was gleaned from the TREES study results, more updated sources (*i.e.* Google Earth) or areas suggested by national experts (most recent areas of degradation). The availability of these types of high resolution images is low in areas of high probability of cloud cover or low economic potential, and therefore we had to rely on several satellites. In particular, we searched for images from Quickbird and Worldview-2 satellites, using the web interface of EUSI, and from IKONOS and Geoeye-1, from EGEOS.

These satellite data with a spatial resolution less than or equal to a metre give a highly detailed view of the target areas, but they are relatively expensive and cover small areas. We selected fourteen images of 7x7 km size located in different biomes and distributed across the country for the year 2010. They belong to the same season as the corresponding RapidEye images, always choosing the closest date available, and when possible, we obtained a second image for the year 2011, so as to be able to review evidence of forest degradation processes (Table 2).

Table 2: Characteristics of the very high spatial resolution images acquired for the project**:** corresponding TREES box (named by the intersected geographic latitude and longitude degrees at its central point), closest location, biome, date and satellite for the year 2010, and date and satellite for 2011. WV-2: Worldview 2, GE-1: Geoeye 1, IK: IKONOS, QB: Quickbird, - : no image for that date.

| TREES box | Location | Biome | 2010 date | 2010 satellite | 2011 date | 2011 satellite |
|---|---|---|---|---|---|---|
| S11E39 | Luatala | Tropical moist deciduous forest | 5-Aug-2010 | WV-2 | 2-Aug-2011 | WV-2 |
| S7E39 | Kisarawi | Tropical rainforest | 11-June-2010 | WV-2 | - | - |
| S8E39 | Ikiwiri | Tropical moist deciduous forest | 9-May-2010 | GE-1 | 11-Jul-2011 | GE-1 |
| S7E36 | Mtera | Tropical shrubland | 4-Sep-2010 | WV-2 | 6-Sep-2011 | IKONOS-2 |
| S5E38 | Mkokoni | Tropical shrubland | 27-Nov-2010 | IK | - | - |
| S6E34 | Mgandu (west of) | Tropical dry forest | 12-April-2010 | GE-1 | - | - |
| S5E30 | Kazuramimba | Tropical moist deciduous forest | 15-Jul-2010 | GE-1 | 1-Jun-2011 | GE-1 |
| S9E34 | Ikuwo (south of) | Tropical mountain system | 17-Dec-2010 | WV-2 | 2-Sep-2011 | GE-1 |
| S8E36 | Mlolo | Tropical mountain system | - | - | 31-Oct-2011 | IK |
| S11E38 | Ruanda | Tropical dry forest | 19-Jun-2010 | GE-1 | 26-Oct-2011 | GE-1 |
| S5E34 | Mgongila | Tropical shrubland | 3-Jul-2010 | QB | 12-Aug-2011 | WV-2 |
| S10E35 | Mahanje (west of) | Tropical moist deciduous forest | 13-Oct-2010 | GE-1 | 3-Oct-2011 | WV-2 |
| S11E35 | Mbinga (east of) | Tropical moist deciduous forest | 3-Nov-2010 | WV-2 | 25-Sep-2011 | WV-2 |
| S5E35 | Misughaa | Tropical shrubland | 21-Aug-2010 | QB | - | - |

These images were used to provide information on the structure of different forest types across the country in different ecoregions to aid in image interpretation.

#### *2.1.2.1 Selection of general field sites*

From the above mentioned fourteen sites covered by high spatial resolution satellite data ('reference sites'), four were selected for field visits ('general and primary sites') according to the accessibility by roads and paths. They were chosen so as to characterise the main forest domains of Tanzania: tropical rainforest, tropical moist deciduous forest, tropical shrubland and tropical dry forest, and correspond to the TREE boxes (LAT-LONG) S7E39, S8E39, S7E36 and S6E34 respectively.

Figure 3 shows the location of all the sites. Note that very few satellite images were available for the northern part of the country due to frequent cloud cover and low image acquisition.

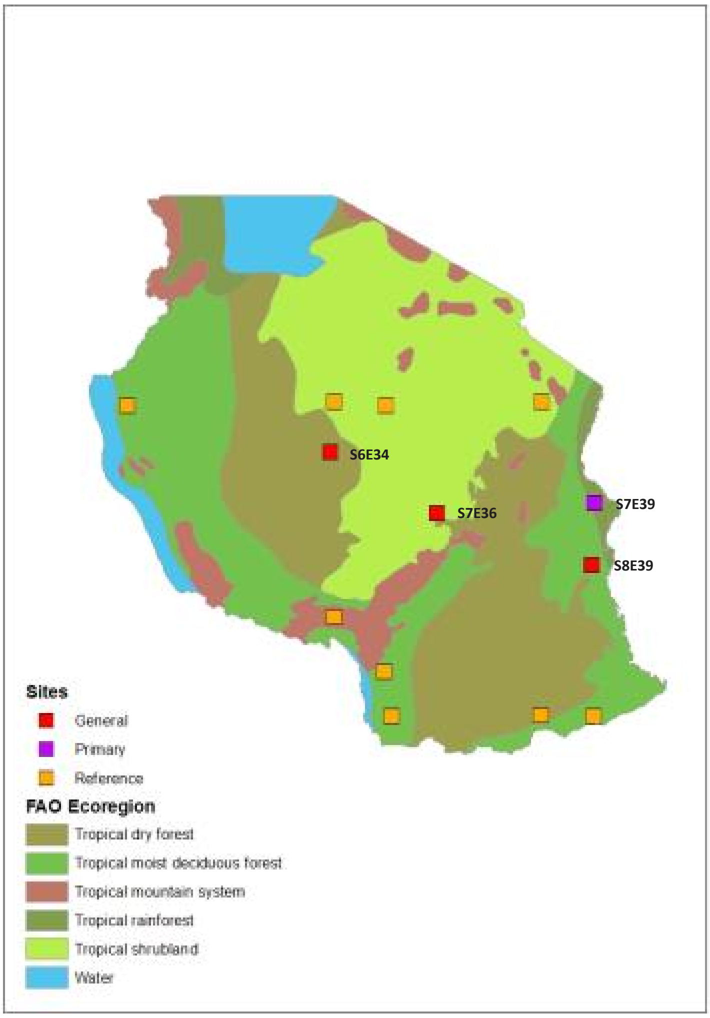


The very high resolution images selected for the general and primary field sites were also used to support the field visits and the selection of the plots.

Figure 3: Location of the field sites in relation to the FAO ecoregion map**.** In yellow all the 'reference sites' covered by very high spatial resolution images, in red those selected as 'general sites', and in purple the 'primary site'.

## 2.2 Primary field site

To select our primary field site we looked for a location where we could rely on logistical support from the NAFORMA field team. The site corresponding to the TREES box S7E39, in the forest of the Pugu hills, near the town of Kisarawe and the closest to Dar es Salaam, fulfilled this condition. Initial examination of available remote sensing data (Landsat, RapidEye and WorldView-2) showed forests in different stages of maturity and degradation.

### 2.2.1 Site description

The TREES sample site (20x20 km) centred at 7°S 39°E, suffered a forest fragmentation of 3.4% of the area between 1990 and 2000 (Bodart *et al*. 2013). More precisely we concentrated our study area on a smaller 7x7 km window centred at 6.91°S 39.06°E, covered by a Worldview-2 satellite subset image. The area is located in the administrative region of Pwani, district of Kisarawe. At its centre is located the town of Kisarawe, at less than 29 km from the city of Dar es Salaam. The Dar es

Salaam-Maneromango road that passes through Kisarawe town is the main route that links the settlements in Kisarawe district with Dar es Salaam.

The site belongs to the Zanzibar-Inhambane ecoregion, which covers the coastal belt of East Tanzania (see Figure 2), in the moist and dry lowland area of the country, and its vegetation is characterized by humid tropical rainforest (see Figure 3). Most of the land is below 200 m and the rainfall is between 800 and 1200 mm per year[3] with a well-defined dry season which runs from mid-June until end of September[4]. The mean annual temperature is 26 °C. Forest is the most widespread climax vegetation, but has been largely replaced by secondary wooded grassland and cultivation. There are also extensive areas of scrub forest and edaphic grassland, and smaller areas of transition woodland, bushland and thicket. The forest is rich in species and difficult to classify (White 1983).

The North-Eastern part of the study area includes a section of the Pugu Forest Reserve, and the South-Western part a section of the Kazimzumbwe Forest Reserve. The rest of the area is composed by bushland with emergent trees mixed with croplands (N-W), mixed crops (S-W) and woodland with scattered crops and tree plantations (S-E) (see Figure 5). The forest reserves contain two main vegetation types: moist forest, remaining primarily only on hillsides, and impenetrable thickets.

According to the Huntings vegetation map (1996) there have been some changes in the land use, mainly the intrusion of agriculture into the Pugu Forest Reserve and Kazimzumbwe Forest Reserve on their western boundaries. The dynamics in these forest reserves are the result of the population growth in the surrounding communities and the expansion of the city of Dar es Salaam. This has brought on the conversion of forest areas into settlements and agriculture in the surrounding areas and to the unsustainable harvesting of forest product by illegal activities within the forest reserves (logging, charcoal burning, timber sawing) to meet the demands of the population (Mdemu *et al*. 2012).

In both forest reserves there is evidence of forest degradation. The main cause of forest degradation is the extraction of fuel wood and charcoal production. In Tanzania firewood and charcoal account for over 75% of the total energy use, mainly for household cooking (Mwampamba 2007). This seems to be the main driver that has converted former lowland forest into shrub formations. During the field survey the presence of charcoal kilns, and charcoal and fuel wood transport (in both heavy vehicles and bicycles) and markets were frequently observed (Figure 4).


Figure 4: Example of a charcoal kiln (left) and charcoal transport (right) in Kisarawe.

[3] Derived from Climatic zones from FAO forestry country information (Ref. page 67).
[4] Derived from Climatic diagrams from Cisgrasp (Ref. page 68).

#### 2.2.2 Worldview-2 image specifications

Satellite imagery for the primary field site was acquired by the Worldview-2 optical satellite sensor on the 11th of June 2010. The satellite was launched in October 2009, has a swath width of 16.4 km and a revisit frequency of 1.1 days. The sensor records data in the blue (0.45-0.51 µm), green (0.51-0.58 µm), red (0.63-0.69 µm) and near-infrared (0.77-0.89 µm) spectral bands at a panchromatic spatial resolution of 0.46 m.

The level 1 image data were geometrically corrected in ERDAS IMAGINE (ERDAS 2002) using Rational Polynomial Coefficients (RPCs) generated from the RPB file supplied with the data. GPS track data collected from a preliminary field visit in 2011 were overlaid on the corrected image to assess the geolocation accuracy. The GPS track and the roads and paths in the image were found to match within 3 m.

Figure 5 shows a true colour composite of the Worldview-2 image covering the primary field site with the approximate limits of the forest reserves overlaid. Three main areas of degraded forest can be discerned in the Pugu Reserve, north (1) and south (2) of the main highway, and in the Kazimzumbwi forest reserve (3).

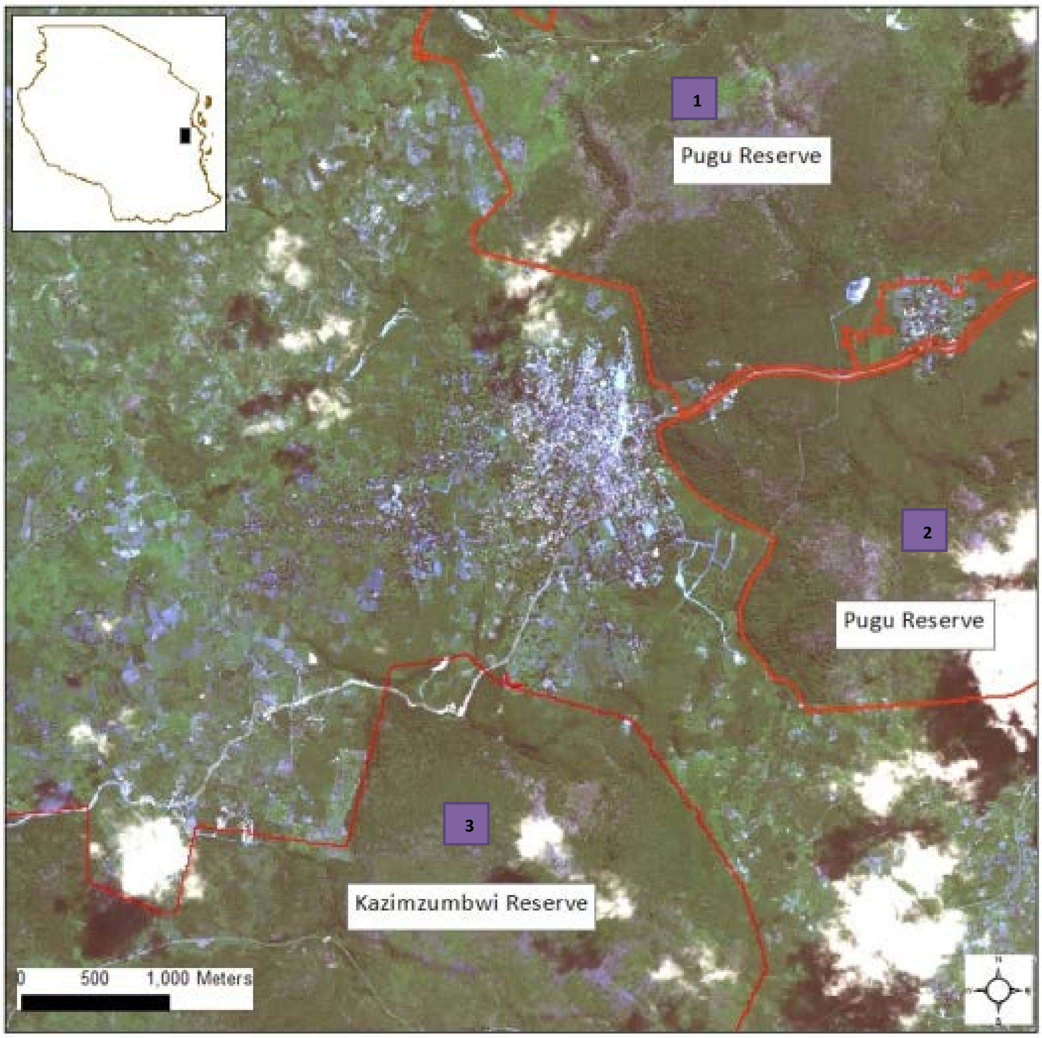


Figure 5: Worldview-2 image (7x7 km) of the primary filed site. In the centre there is the town of Kisarawe, at N-E the Pugu Forest Reserve and at S-W the Kazimzumbwe Forest Reserve. The limits of the forest reserves are approximated. The purple squares indicate three main areas of forest degradation.

# 3. Design of field survey

The design of the field survey implied the following decisions:

1) The measurements - *What do we need to measure?*
2) The sampling method - *Which strategy? Which units?*
*3)* The plot selection - *How many? How distributed?*
4) The required equipment and materials
5) And finally, the practical (logistic and legal) considerations to make the field survey possible and secure.

## 3.1 Field measurements

Our field survey needs to conform to the criteria set out for a future REDD+ monitoring system. However, as yet there is no consensus on the definition of forest degradation, and in consequence, in the way it should be measured and monitored.

Apart from the general definition of forest degradation from the UNFCCC (section 1.2), international organizations such as FAO, IPCC, ITTO, CBD or IUFRO have also defined forest degradation with more or less levels of detail (FAO 2007). As a compromise, we have considered forest degradation as *a long-term loss of productivity, this is, the capacity to provide goods and services, which occurs with a negative change in the structure, which implies a canopy and carbon stock reduction, induced by human activities*. In Tanzania the main ecosystem service provided by the forest are fuel wood and charcoal for energy use.

According to these definitions, to monitor forest degradation we have to assess changes in vegetation type, canopy cover, carbon stock, biodiversity, and presence of human disturbances. To simplify the monitoring of the changes, we needed to establish thematic or quantitative classifications for each of these characteristics, taking into account the national definition of forest adopted by Tanzania in the national REDD strategy (section 1.3)[5].

### 3.1.1 Vegetation type

We developed a vegetation classification scheme that takes into account the national (NAFORMA) classification. The classification is purely physiognomic, which means that discrimination between vegetation types is based on relative appearance, in terms of strata, canopy closure, stature and relative composition of trees, bushes and grass (NAFORMA 2010a), and therefore is appropriate for mapping with remote sensing. The main four classes: forest, woodland, bushland and 'other' are characterised by:

- Forest: three canopy layers (emergent, main and regenerative) and more than 80% of the canopy is covered by trees higher than 5 m. The tropical humid forest is characterised by a full crown cover. In this type of forest, if the canopy cover is higher than 90% it will be considered closed, if less than 90% probably degraded.
- Woodland: two strata (one has trees with normally single stems, from which timber products can be extracted, and the other usually grassland) and the canopy cover is between 20 and 80%. If the canopy cover is higher than 40% it will be considered closed, if less than 40% open.

[5] Possibly under review at the time of writing.

- Bushland and shrubs: a wide range of canopy densities and a height of less than 5 m. Multi-stemmed plants from a single root base are predominant, with the possibility of emergent trees.
- Other classes: include bare soil, grassland, urban area, water and cultivated land.

The main difference between this scheme and the NAFORMA classification is the minimum canopy cover of forest, in our case needs to be consistent with remote sensing data for the humid forest. We have defined this as 80% cover. Table 3 shows the main characteristics of the vegetation classes.

Table 3: Characterization of the main vegetation classes (forest, woodland and bushland) according to number of layers, canopy cover, height and number of stems.

| | Layers | Canopy cover | | Height | N°. stems | Other characteristics |
|---|---|---|---|---|---|---|
| **Forest** | 3 | 80-100% | >90% intact | >5 m | Single | *The tropical humid forest has full crown cover |
| | | | <90% degraded* | | | |
| **Woodland** | 2 | 20-80% | >40% closed | >5 m | Single | One strata composed by trees with single stems |
| | | | <40% open | | | |
| **Bushland** | 1 | Wide range | dense | <5 m | Multi | Possible presence of emergent trees |
| | | | sparse | | | |

Figure 6 shows some examples of vegetation types as imaged by the Worldview-2 satellite. The different classes have not only different percentages of vegetation cover, but also different reflectance (colour) and spatial distribution (texture) properties that can be observed at this high spatial resolution. The latter properties are related with the structure, composition and maturity of the vegetation. For example, in a mature humid forest (top left picture, Figure 6) the crowns of the emergent trees can be well differentiated and project a shadow over the main canopy layer. In the study area degradation usually starts when these larger trees are extracted for fuel wood or timber, leaving holes in the forest canopy (top right picture, Figure 6). If degradation continues, the layer of larger trees is further depleted (*e.g.* for fuel wood or charcoal production) and in a short time a homogeneous layer of shrubland will cover the area (bottom left picture, Figure 6).

To aid in the vegetation classification of the image, we also characterized the undergrowth vegetation type with the following classes: no vegetation, bushes, grass, herbs and new tree regeneration (regrowth).

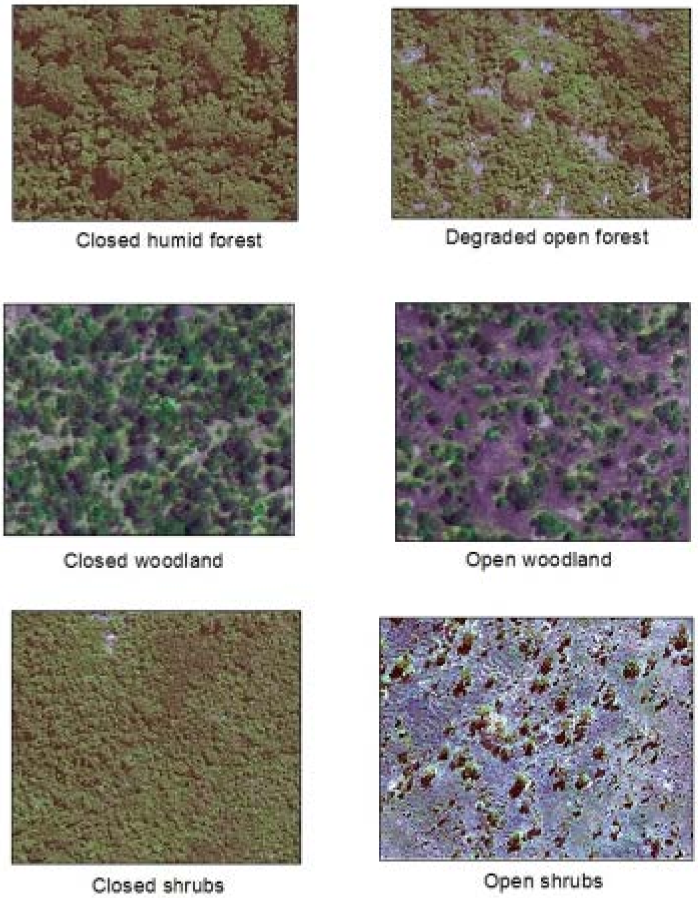


Figure 6: Examples of vegetation classes extracted from Worldview-2 images.

### 3.1.2 Canopy cover

The vegetation classes with woody biomass (forest and woodland) were sub-divided in classes according to the percentage of canopy cover. We set the ranges as <20%, 20-40%, 40-80%, 80-90% and >90%.

### 3.1.3 Carbon stock

Carbon content of vegetation biomass is quite constant across a wide variety of species. It is almost always found to be between 45 and 50% by oven-dry mass (Magnussen *et al*. 2004). The carbon stored in the aboveground living biomass of trees is typically the largest pool (except for peat swamp areas in South East Asia) and the most directly affected by deforestation and degradation in forest areas. The aboveground living biomass is composed of three sub-pools: bole, branches and crown. The bole represents the greatest volume and has the highest carbon density (closely followed by the branches). In tropical rainforest it has been calculated that the total aboveground biomass of a tree can be estimated with high accuracy as an allometric equation with the bole volume as single variable (Eckert, 2012).

Therefore, to estimate the aboveground biomass of a forest, apart from the area covered by woody vegetation, we need to know the volume of the trunks, which can be estimated from the diameter at breast height and the height of the trees. These two variables are generally correlated for a single type of forest, so sometimes one of them can be enough. In our classification, woody vegetation was then sub-divided according to diameter at breast height (DBH), height and the resulting aboveground biomass (AGB) in the following ranges shown in Table 4. In an attempt to be more precise in the estimation of the biomass, we aimed to measure also the crown diameter and tree height.

Table 4: Classes of woody vegetation according to height, diameter at breast height (DBH) and aboveground biomass (AGB).

| Height (m) | | DBH (cm) | AGB tC/ha |
|---|---|---|---|
| <2 | Shrub | <5 | 0-5 |
| >2 | | 5-10 | 6-20 |
| 5-10 | Low forest | 10-20 | 21-50 |
| 10-15 | Medium forest | 20-40 | 51-100 |
| >15 | High forest | >40 | >100 |

#### 3.1.4 Biodiversity

The quality of the wood in a forest for fuel and charcoal production is related to the species and the diversity of trees. Therefore biodiversity indices were calculated.

#### 3.1.5 Natural or human disturbance

In forests with evidence of degradation, the possible cause of the damage (natural or human) was recorded. If due to human impact, the specific human activity (selective cutting, clear felling, timber sawing, charcoal production, burning or agricultural clearance) was also recorded.

### 3.1 Sampling method

A number of different approaches can be taken for the collection of field data (plots, transects etc.) with different sampling strategies (systematic, stratified, random, targeted...) depending on the country ecosystems and information needs (Condit 1998). The number of sampling units will depend on the desired or required statistical robustness of the results and the available financial and human resources.

In our case, the plot sample design was aimed to be compatible with that of NAFORMA. For this reason the sampling units had the same shape, circular plots, so the computation of the field measurements was similar. Transects were not considered, as in any case, displacement through the humid forest can be difficult. As already stated, the objective of the sampling was to characterise the main vegetation types. Therefore the plots were selected as being representative of homogeneous areas of the same forest type.

In a field mission of limited duration, the sampling units need to be targeted, so as to ensure that the main variations in the target thematic are covered with a maximum efficiency. To achieve this, the plots must be located in areas of easy access (proximity to roads), but not so much as to be over influenced by human activities, and they must be representative of the main forest classes.

For the same reason, the plot size was determined in order to cover the maximum forest class variation with the minimum feasible area. We opted for a modification of the national protocol, which used a 15 m radius plot measured by a team of eight, and reduced the radius to 10 m to be measured by a team of four (for budget constraints). We did some tests and estimated that we could do 4 plots in a day and 32 plots in total (8 full working days).

### 3.2 Plot selection

The location of the field plots were visually pre-selected in ArcGIS using the very high resolution satellite image according to different texture and colour. A preliminary segmentation of the image was carried out in eCognition software to delimitate the image into landscape units (Figure 7). We used a multi-resolution segmentation algorithm, which minimizes the average heterogeneity of the image objects according to its spectral information and spatial homogeneity. We gave an importance weight of 20% to the first and 80% to the second criteria, to avoid highly fractured image object results which can result from a strongly textured data (Trimble 2011), as with the pan-sharpened 0.46 m spatial resolution Worldview-2 image.

The resulting segments had different size, according to homogeneity, and a mean mapping unit of 0.5 ha (with a standard deviation of 0.4 ha), in accordance with the national forest area definition. Potential plots had to fall inside segments which fulfilled three conditions: 1) to have a homogeneous texture and colour in all its area, 2) to be close to and accessible from a road or foot path and 3) to have no cloud cover.

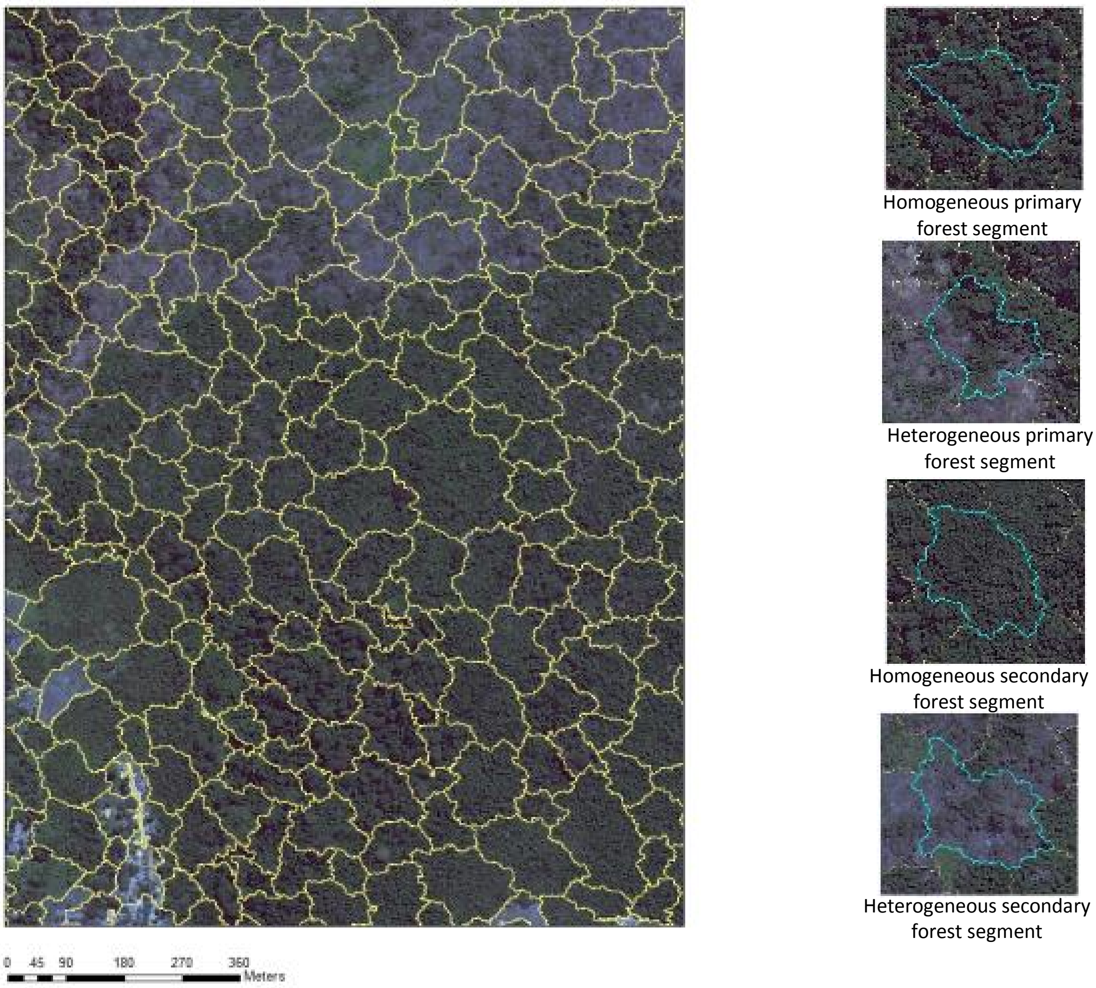


Figure 7: Segmentation of a Worldview-2 satellite image subset (1.0 x 1.2 km) for the selection of potential plot locations. On the right, examples of homogeneous segments with primary and secondary forests (suitable for plot selection) and heterogeneous segments with primary and secondary forests (not preferred for plot selection).

The potential plots were classified into different strata of vegetation type according to Table 3. The stratification by forest type increases survey efficiency by reducing unnecessary sampling while ensuring that major vegetation variations of vegetation type are captured. When implementing the field survey, not all the potential plots can be measured for many reasons (accessibility, land cover change since image acquisition …), but it is important to maintain a well-balanced number of plots per strata to obtain a good diversity of vegetation types.

### 3.3 Field documents

Two types of documents needed to be prepared for the mission, orthophoto maps and the field forms. The first to aid in the location of the plots and the second to record the field observations and measurements.

#### 3.3.1 Orthomaps

In the absence of local topographic maps, we produced orthomaps from the very high resolution images to locate and navigate to plot locations in the field. The maps for the study area were derived from the geo-corrected Worldview-2 image at a scale of 1:5,000, with the reference grid set out in metres for easy calculation of distances in the field. The Building Map Book from ArcGIS was used to divide the full image into sections and create a series of map pages. Figure 8 shows an example of an orthomap sheet of our study area. The maps were then covered in plastic for use in the field.

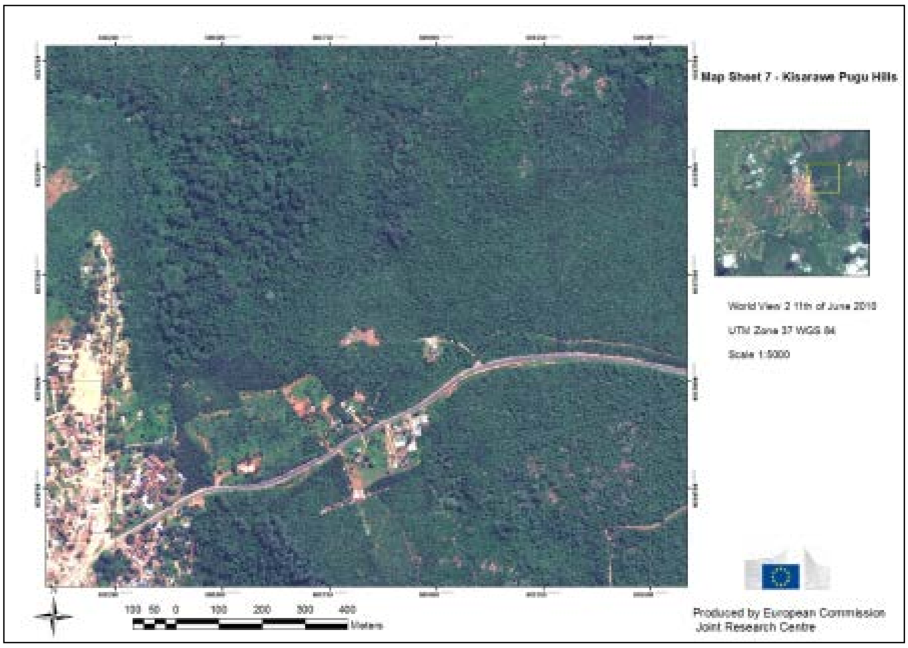


Figure 8: Example of an orthomap sheet of the Kisarawe study area, covering part of the Pugu Forest Reserve (area in the yellow square on the full map at the right), based on a Worldview-2 satellite image.

#### 3.3.2 Field forms

Field report forms were prepared in Excel for recording the plot data to be collected during the field survey. The field forms covered all the observation and measurement information needed as already outlined in section *3.1 Field measurements*. Although it is possible to record directly into the computer, it was deemed prudent to ensure that a paper copy existed, and also it was found difficult recording directly into the computer in the field. The field forms models are shown in the Annex.

### 3.4 Logistical information and official permission

With the collaboration of the country partner (NAFORMA) the timing, costs and logistical considerations were evaluated. We collected information on roads, route times, possible bottlenecks (especially when entering a major city), the official *per diem* rates for hiring local rangers, drivers and botanists, areas of restricted access (*e.g.* military areas), and estimated transport costs (car and fuel). From the two weeks of the main field mission (2012), one week was allocated for field visits to the general field sites and one week for intensive field survey in the primary field site. The periods selected to carry out the field work corresponded to the dry season in Tanzania.

The liaison with the forest services and authorities at both national and local levels is an essential part of the process, not only for logistical, but also for security and legal reasons. In a majority of countries no field survey can be carried out without official permission. In our case, a research permit was required from the national scientific committee, the Tanzania Commission for Science and Technology (COSTECH), along with visits to the district council and forest office for permission to visit forest areas. Through the collaboration with NAFORMA and UN-REDD we acquired the research permits and made appointments with the national forestry hierarchy. Our counterparts also ensured that the local forest managers of our test sites were aware of our mission, and arranged to provide us with local forest rangers. At the same time, the local representatives of our own services, in the EU delegation, were consulted and informed of all the activities.

# 4. Implementation of the field survey

The implementation of the field survey consisted of three main parts: i) navigation to the plots, ii) field measurements and iii) recording of the data. Before starting all the field equipment and the crew required was tested, assessed and assured.

## 4.1 Navigation to plot sites and collection of waypoints

The plot locations selected in ArcGIS (as described in section *3.3 Plot selection*) were printed on the orthomaps. They were also converted to KMZ format for use in Google Earth, and their coordinates uploaded into a GPS. Using internet access we viewed the target locations in Google Earth before visiting the field. This process stores the available image in the Google Earth cache. Alternatively a 3G key can be used to have real time access to Google Earth if telephone access is assured. In the car, with the GPS connected to the computer, the 'Realtime Tracking' utility in Google Earth was used to reach the points closer to the plots (Figure 9)[6]. One has to be careful about totally relying on this method, as at times the connection with the GPS can be lost and very high resolution data is not always available for all locations. In which case local topographic maps, where available, have to be used. In the field the orthomaps and the GPS were used to locate the plots.

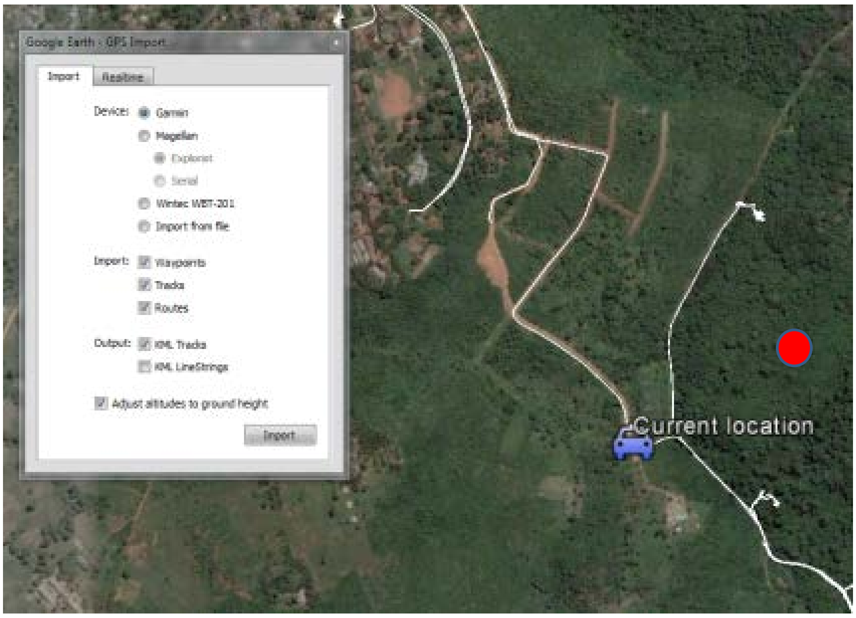


Figure 9: Visualisation of the 'Realtime Tracking' utility in Google Earth to navigate to the plots. The image where the plots are located needs to be viewed when internet connection is available so as to cache the images.

[6] ArcGIS has a similar real time GPS link utility, however the GPS needs to be connected through a COM port (rather than a USB) and not all new computers are equipped with this. The problem can be solved by emulating a COM port connection and linking your USB connection through this virtual COM. Some GPS device manufacturers provide drivers to map the USB connection to a virtual COM port. Bluetooth devices also can be configured to use a virtual COM port. For more information on how to connect a USB GPS handheld device to ArcGIS Desktop, see:
http://esriaustraliatechblog.wordpress.com/2011/09/01/how-to-connect-your-usb-gps-handheld-device-to-arcgis-desktop/

The GPS was put on ‘tracking’ mode for the duration of the field visits. Care is needed to ensure the sampling rate is high enough to capture all movements, especially when using transport (Figure 10). However, high sampling rates can quickly fill the GPS memory storage card. Along the way, waypoints with associated photographs were collected at points of interest to aid in image classification and at distinct land marks (*e.g.* road intersections) for ensuring the geometric fidelity of the satellite imagery. It is important before starting the field visits that the times on the GPS and photo camera are synchronised. The location of the waypoints was spontaneous and not pre-selected as in the case of the plots. Waypoint coordinates, photograph ID numbers and notes were recorded on the *Waypoint form* (Annex table 1).

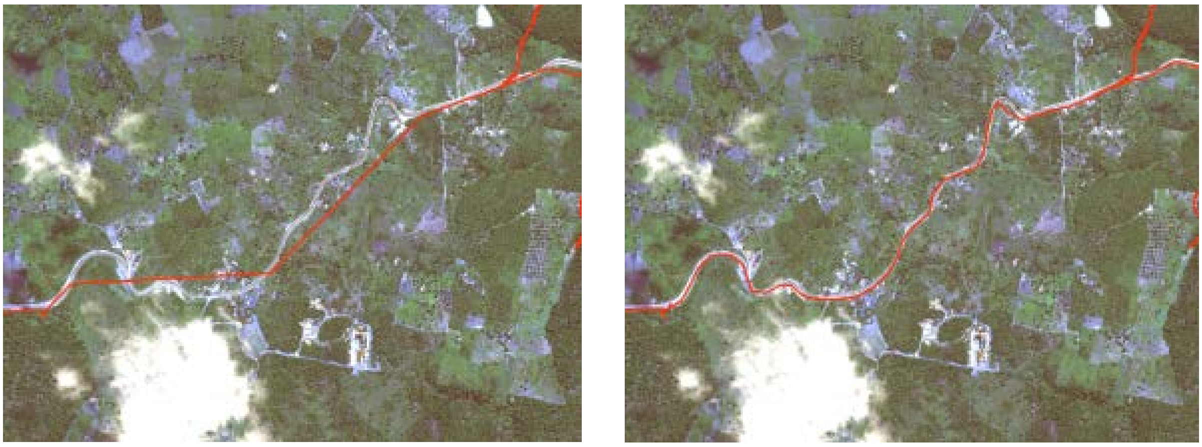

Figure 10: Example of GPS tracking at two different recording rates. The trail on the left was recorded at one minute intervals and the one on the right at one second intervals.

### 4.2 Plot measurement protocol

A consistent protocol was used to measure all plots, following all steps in a set sequence, as laid out in Table 5. Each member of the field crew was assigned a particular task. In the following sections the protocol steps are described with more detail. First, the tasks related to the retrieval of plot general information, and second, the measurements of trees inside the plot.

Table 5: Steps of the plot measurement protocol with the data to be recorded and equipment needed.

| | Task / measure | Record | Equipment |
|---|---|---|---|
| 1 | Locate and mark plot centre | Plot reference and coordinates | Stake, GPS |
| 2 | Delimit plot area (set out 10m length ropes in four cardinal directions) | | Four ropes of 10 m, four stakes, a compass |
| 3 | Take photos of plot centre and at the four cardinal directions | Photo numbers from camera | Photo camera |
| 4 | Slope | Percent slope | Clinometer |
| 5 | Canopy cover at plot centre and at the cardinal directions | Percentage canopy cover | Spherical densiometer |
| 6 | Describe the plot | Vegetation and undergrowth type, damage and human impact | Field codes, plot forms |
| 7 | Mark trees by quadrant | Tree numbers | Tags and marker pen |
| 8 | Tree DBH | Stem DBH | Diameter tape |
| 9 | Tree height and location | Tree total height, distance and azimuth to plot centre | Laser rangefinder |
| 10 | Record tree species | Vernacular and botanic species names | NAFORMA species list |

### 4.2.1 General measurements and information

The identification and characterization of each plot was made by filling the *Plot form* (Annex table 2). Before starting with the observations and measurements, a plot identification number, date, starting time of the field work at the plot, and a description of the area were recorded.

#### *4.2.1.1 Plot centre location and area delimitation*

The plot centre was marked with a stake and the location recorded with the use of a **GARMIN GPSMAP 60CSx**, in WGS84 coordinates and datum, and UTM projection in metres to facilitate the location on the map. At this point, a reference photograph with the plot identification number was taken.

To delimit the area and mark the cardinal directions, four ropes of 10 m each tied to a stake were run out from the centre in the cardinal directions using a compass and fixed in the ground. Four photographs were taken at the centre addressing the cardinal directions, always proceeding in the sequence N-E-S-W, to help the image interpretation (Figure 11).

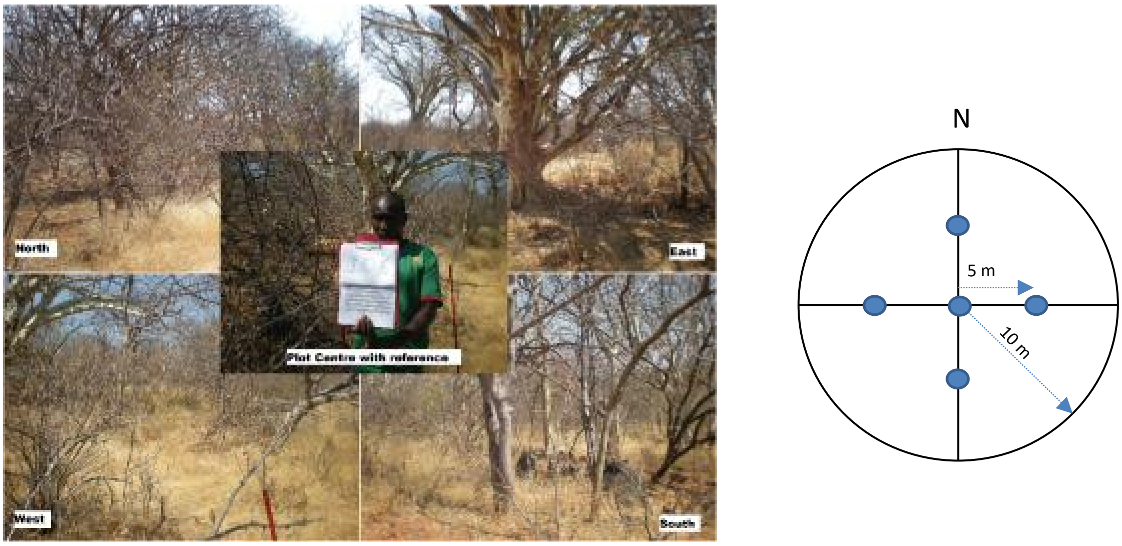


Figure 11: Example of photos taken at a plot centre, with the plot identification number, and in the cardinal directions (left) and a scheme of a plot (right). The blue circles indicate the points where the canopy cover was measured.

#### *4.2.1.2 Slope*

When the plot is on sloping ground, the slope needs to be accounted for the calculation of the area. The distance between two points measured along a slope terrain is always longer than the equivalent on a flat terrain. The distance must be multiplied by a factor that corresponds to the inclination in order to obtain the equivalent horizontal one.

Horizontal distance = slope distance x cos ($\alpha$), where $\alpha$ = inclination angle in

The area of the plots on slope terrain can be delimited to be equivalent to that on a flat terrain directly in the field. For this, the radius of the plots must be adjusted to measure a fixed area vertically projected on the horizontal plane, using the following equation:

$$\text{Radius} = \sqrt{\text{area} / (\pi \times \cos(\alpha))} = \sqrt{\pi \times r^2 / (\pi \times \cos(\alpha))} = r / \sqrt{\cos(\alpha)}$$, where $\alpha$ = inclination angle in degrees

The slope was measured in percentage using a **Suunto hypsometer**, and for all slopes above or equal to 5% the plot area was corrected by adjusting the radius. A table with the corrected plot radii according to the slope is presented in Annex table 10. Alternatively, slope can also be measured with a clinometer or a laser rangefinder (see *4.2.2.2 Tree height* and Annex figure 1).

#### *4.2.1.3 Canopy cover*

The canopy cover of the plot was measured at five points: at the plot centre and at 5 m distance from the plot centre in the four cardinal directions (Figure 11, right picture), with a **spherical densitometer**. This instrument has a reflective spherical surface divided into a grid of 24 squares (Figure 12). When the instrument is taken under the forest canopy, the reflection of the tree crowns or the sky overhead can be seen in the mirror. The canopy cover is estimated based on the proportion of the mirror surface covered by vegetation.

Figure 12: Canopy cover measurement with a spherical densitometer (enlarged on the right).

Each square in the grid represents an area of canopy cover (filled squares) or canopy opening (unfilled squares). The actual canopy cover is computed by the average number of filled squares multiplied by a factor:

Canopy coverage (%) = average number of squares reflecting tree crown x 4.17

The densitometer has to be held far from the body horizontally at shoulder height (approximately 1.6 m) and always directing north. To ensure consistency, each member of the crew needs to train in the use of the instrument.

#### *4.2.1.4 Vegetation and undergrowth class*

The vegetation and undergrowth classes were recorded according to the vegetation classification described in *3.1.1 Vegetation type* (codes in Annex table 5 and Annex table 6 respectively).

#### *4.2.1.5 Damage and human impact*

Possible causes of damage (natural or human induced) and human impact in the forest areas were recorded using a list of codes (Annex table 7 and Annex table 8).

### 4.2.2 Tree measurements

Proceeding by quadrant (from northeast in clockwise-direction), all 'trees' were marked with a tape on which a sequential number was written. If a tree had multiple stems that started below 1.3 m height, these were considered individual trees to be measured. The sequential numbers along with the measurements were registered on the *Tree form* (Annex table 3).

#### *4.2.2.1 Tree diameter (DBH)*

The tree diameter at breast height (DBH) was measured on the trunk at 1.3 m height above the ground with a **diameter tape**. This has one side with a centimetre scale and the other with the direct conversion into diameter. Only the stems with a DBH greater than 5 cm were recorded. A 1.3 m stick was used to determine the breast height of the trunk from the ground level (Figure 13). The diameter should be measured always perpendicular to the trunk.

Figure 13: Tree DBH measurement with a 1.3 m stick and a diameter tape (enlarged on the right).

When measuring the DBH some particular measurement cases can be found, the most common are:

a) Trees leaning on flat terrain. The breast height is measured at the side where the tree leans.
b) Trees on slopes (up or down). The breast height is measured at the upper part of the slope.
c) Forked trees where the fork (the point where the trunk is divided) originates below 1.3 m height. Each stem reaching the 5 cm diameter is considered as a stem to be measured, and the diameter is measured at 1.3 m height.
d) Forked trees where the fork originates at 1.3 m or higher. The tree is counted as a single tree and the diameter is measured below the fork intersection point at 1.3 m, or just below the bulge that could influence the measurement.

### *4.2.2.2 Tree height*

The height of all trees with a DBH >5cm was measured at the top of the crown with a **TruPulse 360° Laser Rangefinder** (Figure 14). There are many other instruments to measure tree height, *e.g.* the hypsometer that was used for measuring the slope.

Figure 14: Tree height measurement with a TruPulse 360° laser rangefinder and Trimble Recon data logger (enlarged on the right).

Height measurement with the laser rangefinder involves targeting three points on the tree: the base of the trunk, a point at horizontal distance on the tree and the top of the crown. The tree height is calculated by applying the Pythagorean Theorem (Figure 15). In dense canopy cover these measurements are not always possible and the height was estimated visually, averaging the estimation of three persons of the crew; alternatively one can move out of the plot and find the average height from further away.

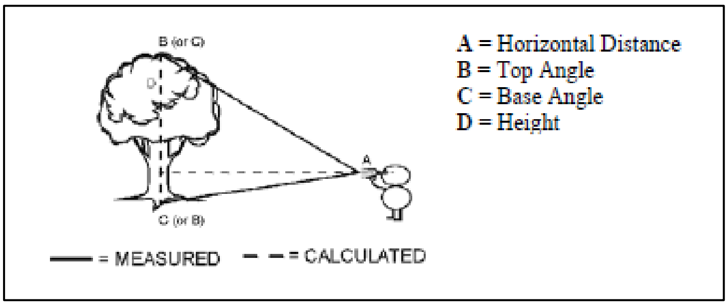


$$D = \sqrt{C^2 + A^2} + \sqrt{B^2 - A^2}$$

Figure 15: Laser rangefinder routine to measure tree height (source: Laser Technology Inc. 2011) and geometry.

#### 4.2.2.3 Tree position

The TruPulse 360° laser rangefinder was also used for obtaining the tree position in the plot, by measuring the distance and azimuth from the plot centre to the tree (Annex figure 1). Before starting the field work, the azimuth measurement of the instrument needs to be calibrated with a conventional compass to align it with true north.

The instrument records data in a text file and is equipped with a Bluetooth to download it to either a data logger (Trimble Recon, Figure 14) or a laptop. The use of the data logger was found to be difficult in the tropics, as sunlight made the screen hard to read. Mapping and data manipulation can be carried out with *MapSmart Field Mapping software*, however, for position within the plot we used a simple Excel file.

#### 4.2.2.4 Crown diameter

Attempts were made to measure crown diameter using the TruPulse 360° Laser Rangefinder, by taking two measures at the widest parts of the crown. However, accurately targeting the outer limits of the crown proved problematic in dense forests.

#### 4.2.2.5 Tree species

The species of all targeted trees were identified by a Tanzania Forest Service staff (Figure 16, left). For the recording of the tree species we were supported by the *NAFORMA Species List* (NAFORMA 2010b), which is available in both Latin and vernacular (local) names. When the species of a tree was uncertain, leaves and fruit were collected for later identification. A simple book was used to keep the collected material along with its tree reference number on the field forms.

#### 4.2.2.6 Stumps

When present stumps were also recorded. DBH (Figure 16, right), height, species and if possible an estimation of the years from cutting were registered in the *Stump form* (Annex table 4). If the stumps were less than 1.3m tall the diameter was measured below the cutting point.

Figure 16: Tree species identification (left) and DBH stump measurement (right).

## 4.3 Data recording and storage

All data (field forms, GPS data and photographs) were reviewed and backed up at the end of each field visit day.

### 4.3.1 Field sheets

It was found important to review the field forms immediately at the end of the day. Small errors and omissions in the forms can be easily rectified shortly after the visit, which is not the case if they are reviewed at later date. Excel sheets were created to enter the data. It is better to create a data input interface in Excel to reduce errors (this is added to the menu by selecting 'Form' under the 'All commands' menu in 'Customizing the Ribbon'). To avoid duplications and spelling inconsistences we used codes for vegetation classes and tree species, which then can be put into text using a lookup table. Four Excel sheets, each one corresponding to a field form (waypoint, plot, tree and stump forms) were used for the following input data:

- *Waypoint sheet:* waypoint ID number, GPS location (Easting and Northing), photo ID number and comments.
- *Plots sheet:* plot number, location, vegetation type, canopy cover, slope, photo ID numbers, damage, etc.
- *Trees sheet:* tree number, stems numbers, position in the plot, height, species, DBH.
- *Stump data:* stump number, height, DBH, species and estimated years from cutting.

Figure 17 shows an example of plot and tree Excel sheet.

| PLOT SHEET | |
|---|---|
| Plot number | 9 |
| Field site | S7E36 |
| Forest /area name | Mtera / Dry |
| Date | 8/7/2012 |
| Time | 11:22 |
| UTM Zone | 36 |
| GPS Coordinates - X | 826321 |
| GPS Coordinates - Y | 9217542 |
| Slope | 5% |
| Photo ID in camara - C | 1056 |
| Photo ID in camera - N | 1057 |
| Photo ID in camera - E | 1058 |
| Photo ID in camera - S | 1059 |
| Photo ID in camera - W | 1060 |
| Canopy cover - C | 17 |
| Canopy cover - N | 7 |
| Canopy cover - E | 21 |
| Canopy cover - S | 6 |
| Canopy cover - W | 9 |
| Canopy cover average | 50% |
| Vegetation type | WO- Woodland open |
| Land use | 6- Grazing land |
| Undergrowth type | 3- Elephant grass |
| Damage *(living trees)* | 0 |
| Severity | |
| Human impact | 2- Selective cutting |
| Estimated time | 1 year |
| Notes | |

| TREE SHEET | | | | | | | | |
|---|---|---|---|---|---|---|---|---|
| Tree n° | Species vernacular name | Species botanic name | Distance (m) | Azimuth (°) | Total height (m) | Stem n° | DBH (cm) | Tree utilities |
| 1 | Moza | *Sterculia africana* | 8 | 81 | 8.7 | 1 | 75 | timber |
| | | | | | | 2 | 26.1 | |
| | | | | | | 3 | 30 | |
| 2 | Boabab | *Adansonia digitata* | 9 | 81 | 8.7 | 1 | 48.1 | food, fodder, rope, twine |
| 3 | Bakchandi | *Commiphora africana* | 8.7 | 146 | 6 | 1 | 11.23 | firewood, resin |
| 4 | | *Commiphora eminii* | 5.9 | 169 | 4.9 | 1 | 22.28 | firewood |
| 5 | | *Lannea fulva* | 5.2 | 2.55 | 8 | 1 | 19.5 | edible fruits, firewood |
| | | | | | | 2 | 15.7 | |
| 6 | | *Commiphora eminii* | 6.9 | 2.76 | 5 | 1 | 6.2 | firewood |
| 7 | | *Catunaregam spinosa* | 7.2 | 2.76 | 5.3 | 1 | 4.2 | medicinal, firewood |
| | | | | | | 2 | 3.9 | |
| 8 | Bakchandi | *Commiphora africana* | 3.6 | 2.76 | 5 | 1 | 8.4 | firewood, resin |
| 9 | | *Commiphora eminii* | 9.6 | 2.9 | 5.8 | 1 | 8.9 | firewood |
| | | | | | | 2 | 8.5 | |
| | | | | | | 3 | 5.7 | |
| | | | | | | 4 | 9.6 | |
| | | | | | | 5 | 6.8 | |
| 10 | Bakchandi | *Commiphora africana* | 10 | 3.34 | 6.5 | 1 | 5.2 | firewood, resin |

Figure 17: Examples of plot (left) and tree (right) Excel sheets for plot number 9.

### 4.3.2 GPS data

GPS data were downloaded at the end of each day's field visit, converted into shapefiles and reviewed in ArcGIS using the *DNR Garmin Application* from Minnesota Department of Natural Resources. This allows the transfer of data between Garmin GPS handheld receivers and various GIS software packages (ArcGIS, Google Earth). It is advisable to retain the original GPX file, as conversion to shapefile can lead to a loss of some attributes. It was also found that saving the track log to a file on the GPS lost frequency resolution of the point data, therefore it is better to download the original track log. A memory card should be added to the GPS to ensure that the track log does not saturate.

### 4.3.3 Photos

Photos were reviewed with the plot forms (photo's ID) to ensure correspondence. On some cameras deleting photographs leads to a renaming of the photo number sequence, which can lead later to confusion. The photos were then geolocated using the *COPIKS PhotoMapper* software, which tags the JPEG files with the GPS locations loaded from the GPX file and exports them to Google Earth display. To ensure smooth linking the camera should have the same time as the GPS. Alternatively, we also used a Lumix DMCTZ30 camera with GPS included. The GPS in the camera takes time to update the GPS position, so care is needed to ensure that the current position reading has been taken before taking a photo. The *COPIKS PhotoMapper* utility also produces KMZ tracks and photolinks for use in Google Earth. For some cameras the downloaded photos may need their suffix changed from 'JPEG' to 'jpeg' for linking in Google Earth. This was done in a small script.

## 4.4 Field crew

To carry out the field survey a minimum of four people are required (in open vegetation three may suffice), apart from the driver. One/two personnel are needed to demark the plot and tag the trees and two personnel to measure and record the data. One of the crew members needs to be able to identify the tree species. Depending on the location and security situation a guard may also be required. The field crew composition could be:

1. Two persons for the measurement and recording data (JRC staff)
2. Botanist/tree identifier
3. Local forester/wildlife guard

## 4.5 Field equipment

The preparation of the field equipment needs to be carefully undertaken, as few in-country resources may be available. Table 6 gives a list of the materials used in the field survey and their application.

All equipment needs to be tested before the field mission. Important issues are:

- Some computer programs and functions need administrative rights to run and install.
- The cameras and GPSs must be set to the same time, so as to allow later geolocation of the photographs.
- Both GPS systems have to be checked for correct datum and sampling rates. We used the WGS84 datum, although local topographic maps are in Arc60 datum. It would be advisable to have a third GPS in the local datum, to enable geolocation matching with national data sets.

- GPS data downloading to the computer should be tested (format, attributes, frequency resolution).
- Extra batteries should be procured for all the instruments, especially important for the equipment not readily available (*e.g.* the laser rangefinder).

Table 6: Equipment and software needed for the field survey and application.

| Equipment and software | Use / Measurement |
|---|---|
| 2 Laptops with ArcGIS, Google Earth, Excel, GPS software (DNR Garmin Application), COPIKS PhotoMapper | Navigation to plot, field data entering, photos and GPS data backup, format conversion and review |
| Transformer 12v - 220v (+ extra one in case it gets overheated) | Use of laptop in vehicle |
| 2 GPS GARMIN GPSmap 60CSx (+ extra batteries and memory card) | Navigation to plot, plot centre location, waypoints and track collection |
| Orthomaps (UTM 1: 5,000) | Plot location in the field |
| 2 Digital cameras (+ extra batteries and memory card) | Plot and waypoints pictures |
| External hard drive | Photos and GPS data backup |
| Marker, paper | Plot identification flipchart for reference photograph |
| Metal poles (x6) of 1.3 m length | Plot centre and boundary marking, tree breast height |
| Compass | Delimitation of plot into 4 cardinal quadrants |
| Ropes (x4) of 10 m length (with a colour sign at 5 m) | Plot boundary marking, canopy cover |
| Densiometer | Canopy cover at 1.6 m |
| *Suunto* hypsometer or clinometer | Slope, (tree height) |
| Field codes | Vegetation and undergrowth type, damage, human impacts |
| Yellow tape and marker | Marking tree numbers |
| Diameter tape | Tree DBH |
| *TruPulse 360°* Laser Rangefinder (+tripod) and data logger (+extra batteries) | Tree location, height, (land slope), (tree crown diameter), data recording |
| Species list (Latin and local names) | Botanist support |
| Field forms, pen | Data recording |
| Writing tablet / pad | Data filling on field forms |
| First aid kit and hospital location | Emergency measures |
| Radio | Field to vehicle communication |
| Bush knife / machete | Vegetation opening for access to the plot |
| Research permit (from national scientific committee) | Visit to forest areas |

## 5. Analysis of field data

The data were first analysed and parameters were computed in order to produce a range of maps useful to forest management and assessing carbon pools.

### 5.1 Waypoints and plots

We collected a total of 184 waypoints and measured a total of 22 plots during the field mission in 2012 (Figure 18); 14 in the primary field site in the humid forest (Figure 19), 4 in the general field sites in the dry and Miombo forests, and 5 in the general field site in the semi-humid forest.

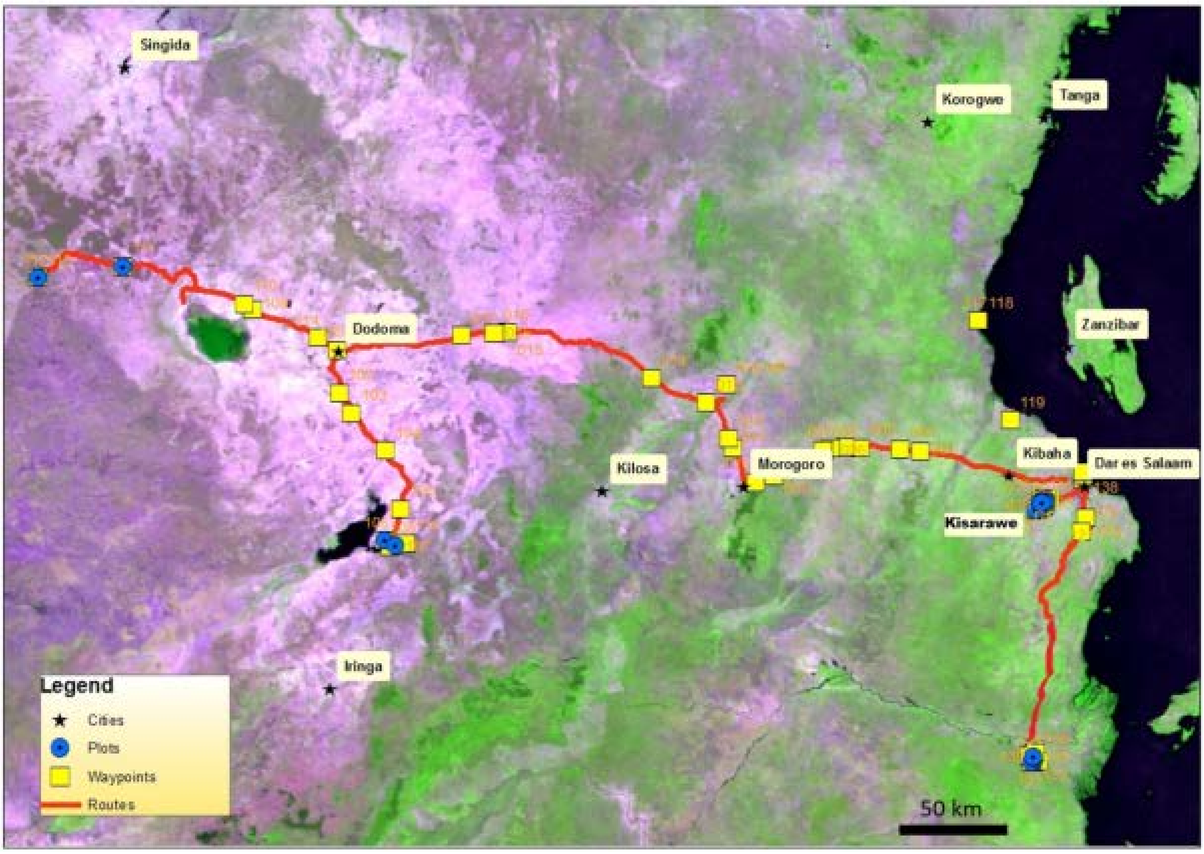


Figure 18: Route followed in the field work of 2012 with waypoints and plots. The two groups of plots on the East belong to the field sites in the humid (North) and the semi-humid (South) forests. The two groups on the West to the field sites in the dry and Miombo forests (respectively from East to West).

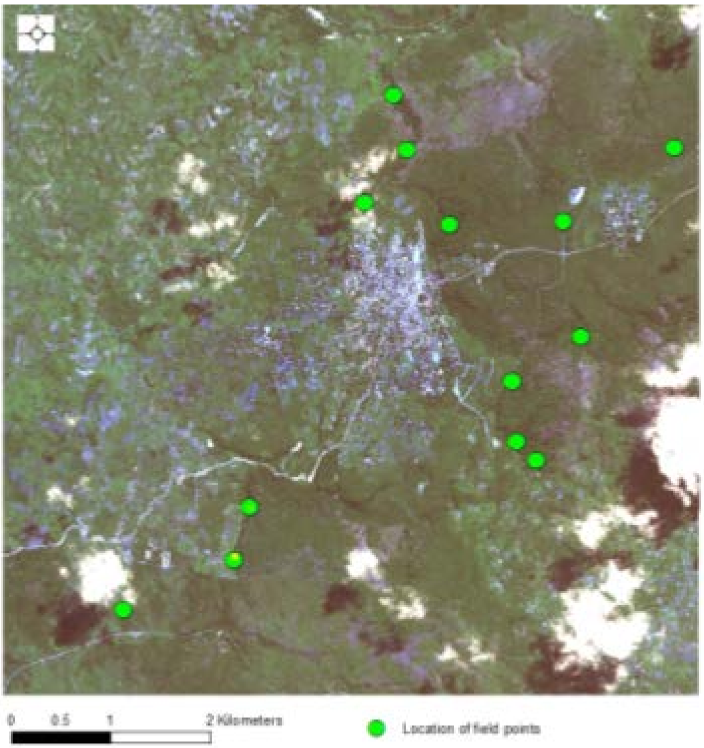


Figure 19: Location of the plots in the primary field site (in Kisarawe).

### 5.2 Plot data calculations

From the original field measurements we calculated the plot parameters described in this section (summarised at the end in Table 7) and produced maps of tree distribution at plot level, changes of which are intended to indicate degradation processes.

#### 5.2.1 Plot corrected area

Ten plots were on slopes with more than 5% of pendent and the radii were adjusted according to Annex table 10 to obtain the equivalent horizontal area as seen in the satellite image.

#### 5.2.2 Average canopy cover

The canopy cover of the plots was computed as the average of the canopy cover measured at five points (centre, north, east, south and west) at 1.6 m height.

#### 5.2.3 Number of woody plants and trees

All the plants with a DBH greater than 5 cm were recorded, but only those plants with a total height greater than 5 m were considered trees in the humid forest.

#### 5.2.4 Basal area

The basal area per ha is the sum of the area of all woody plants at breast height in one hectare. To calculate it all the stems with a DBH >5cm were taken into account. Tropical forests are characterized by having a negative exponential diameter distribution, so that the number of trees decreases with the size of the trees. The stems with a DBH <5cm were not measured to save time, as potentially there are many but represent a low percentage of the biomass. The biomass of these small stems could be estimated approximately 5 % of the total.

Total basal area (BA) in the plot ($cm^2$):

$\sum_{i=1}^{N} \pi * \frac{{dbh_i}^2}{4}$ where $dbh_i$ is the DBH (cm) of plant $i$ and $N$ is the total number of plants.

Basal area per $m^2$:

$\frac{BA}{\pi * R^2}$ where $R$ (m) is the plot radii. The resulting unit is $cm^2/m^2$ or the equivalent $m^2$/ha.

### 5.2.5 Volume

The wood volume is the sum of the volume of all woody plants. In Tanzania there are general equations for predicting tree volumes for tropical dry forests (Chamshama *et al.* 2004, Luoga *et al.* 2002), tropical shrubland (Isango 2007), but not for moist deciduous forest and tropical rainforest. In the absent of a local equation, the volume of a tree is estimated to be the 50% of the cylinder which results from multiplying the basal area and the total height (Henry *et al*. 2011).[7]

Total wood volume (Vol) in the plot ($m^3$):

$\sum_{i=1}^{N} \pi * \frac{dbh_{ix}^2}{4} * H_i * 0.5 * 1/10{,}000$ where $H_i$ is the height (m) of plant $i$, $dbh_{ix}$ the DBH (cm) of stem x of plant $i$, $N$ is the total number of plants and 0.5 is the average form coefficient for conic trees (CIRAD and MAE 2004, in Henry *et al*. 2011).

Wood volume per ha ($m^3$):

$\frac{Vol}{\pi * R^2} * 10{,}000$ where $R$ is the plot radius (m).

### 5.2.6 Aboveground biomass and carbon content

The density of the wood in humid forests is estimated to be a bit higher than in other ecoregions. The most common average wood densities values for tropical tree species in Africa is 0.5-0.79 $t/m^3$ and the mean wood density 0.58 $t/m^3$ (Brown 1997)[8]. The aboveground biomass (AGB) per hectare was calculated as:

AGB (t/ha) = wood volume ($m^3$/ha) * 0.58 ($t/m^3$)

We assume that the carbon content of the biomass is 50% of the dry mass (Magnussen *et al*. 2004). Hence the carbon content of the aboveground biomass (AGC) per hectare was calculated as:

[7] Other empirical analyses indicate that the volume of a tree is between 0.40 and 0.45 times that of an equivalent cylinder, and therefore propose the use of the general equation V=0.42*dbh*H. This is because trees are neither cylinder nor cones, and the volume of a cone is one-third of the volume of a cylinder with the same basal area and height (Magnussen *et al*. 2004).

[8] Other sources propose higher or lower average wood density values. For example, the average wood density given by the Intergovernmental Panel on Climate Change is 0.62 t/m3 (IPCC 2006).

AGC (tC/ha) = AGB (t/ha) * 0.5 (tC/t)

### 5.2.7 Biodiversity indices

Three biodiversity indices were calculated taking into account all woody plants:

- Species diversity index. It gives the diversity of species in relation to the total number of individuals. It is calculated with the simple ratio of the total number of different species (S) to the total number of individuals (N): $\frac{S}{N}$.

- Margalef index. This estimates the total diversity of species based on the numeric distribution of the individuals from different species in function of the total number of individuals. It has the following expression:

  $$I = \frac{S - 1}{\ln N}$$

  where S is the total number of species and N the total number of individuals. Values less than 2.0 are considered being related to areas with low biodiversity (in general as result of anthropogenic effects), and values higher than 5.0 to areas of high biodiversity.

- Shannon Index. Provides an estimate of the relative distribution of species taking into account the number of species (species richness) and the relative quantity of individuals of each of the species (abundance). Its formula is the following:

  $$H = -\sum_{i=1}^{S} pi * \ln_2 pi \text{ ,}$$

  where S is the total number of species and $p_i$ is the relative quantity of the species i, $p_i=(s_i/N)$, where $s_i$ is the number of individuals of the species i and N the total number of individuals of all the species.

### 5.2.8 Plot parameters summary

Table 7: Plot parameters derived from the field measurements.

| Field measurement (units) | Plot parameter (units) | Formula / calculation | |
|---|---|---|---|
| **Slope (%)** | Plot corrected area (m$^2$) | $\pi * R^2$ | R (m) is the corrected radius for slope >5% |
| **Canopy cover (%)** | Average canopy cover (%) | Mean of five measurements (C, N, E, S, W) | |
| **Woody plants count** | N° woody plants | Stems with DBH >5cm | |
| | N° trees | Stems with DBH >5cm and height >5m | |
| **DBH (cm)** | Average DBH (cm) | DBH >5cm | |
| | Standard deviation DBH (cm) | DBH >5cm | |
| | Basal area per ha (m$^2$) | $\sum_{i=1}^{N} \frac{0.785 * dbh_i^2}{\pi * R^2}$ | $dbh_i$ is the DBH (cm) of plant i, N the total number of plants and R (m) the radius |
| **Height (m)** | Average height (m) | DBH >5cm | |
| | Standard deviation height (m) | DBH >5cm | |
| **DBH and height** | Wood volume per ha (m$^3$) | $\sum_{i=1}^{N} \frac{0.392 * H_i * dbh_{ix}^2}{\pi * R^2}$ | $H_i$ is the height (m) of plant i, $dbh_{ix}$ the DBH (cm) of stem x of plant i and R (m) the radius |
| | Aboveground biomass (t/ha) | Wood volume (m$^3$/ha) * wood density (0.5-0.58 t/m$^3$) | |
| | Aboveground carbon content (tC/ha) | Aboveground biomass (t/ha) * carbon content (0.5 tC/t) | |
| **Species** | N° species (S) | N° of different species | |
| | Species diversity index | $\frac{S}{N}$ | S is the total number of species and N the total number of plants |
| | Margalef index | $\frac{S-1}{\ln N}$ | |
| | Shannon index | $-\sum_{i=1}^{S} pi * \ln_2 pi$ | $p_i$ is the relative quantity of specie i, $p_i=(s_i/N)$ where $s_i$ is the number of individuals of species i |
| **Distance (m) and azimuth (°)** | Location (x,y) | X= GPS Easting + sin(α) * d<br><br>Y= GPS Northing + cos(α) * d | α is the azimuth and d the distance from the tree to the GPS |

### 5.2.9 Tree location

The location of each woody plant within the plot was calculated with the distance to the centre of the plot and the azimuth. The GPS coordinates of the plot centre were then used to overlay the plot tree data on the image.

## 5.3 Plot data results

### 5.3.1 Vegetation structure and biomass

For each plot we produced a synthesis of the field data calculations and observations. Table 8 shows the synthesis of all the plots, from the primary field (humid forest) and from the general field sites (dry, semi-humid and Miombo forest). In total they sum up 23 plots, covering a total area of 7.225m$^{2.}$

### 5.3.1 Allometric equations

The number of total stems measured in the humid, dry and semi-humid biomes was 172, 76 and 27 respectively. The relationship between height, H, (m) and DBH (cm) in the humid biome was:

$$H = 11.182 * \ln dbh - 17.323 \; (R^2 = 0.75)$$

This relationship was used to estimate tree height for sites with stumps from trees cut after the satellite image acquisition date (as in plots n$^{o}$7 and n$^{o}$8).

Crown diameter was difficult to measure with the laser rangefinder. Instead, allometric equations were obtained from the literature and adapted to Tanzania (after O'Brien *et al*. 1995).

$$\log(CA) = 1.3 * \log(dbh * 10) - 2.0$$

Ideally by measuring the crown area directly from the image, we could obtain the DBH, which is related to the height for a same type of forest, and therefore the volume.

Table 8: Synthesis of the field data calculations for all the plots.

| Plot no. | Forest type | Location | Vegetation (and degradation) | Longitude DMS | Latitude DMS | Canopy cover (%) | No. of woody species | No. of tree species | Average DBH (cm) | SD DBH (cm) | Basal area per ha ($m^2$) | Average height (m) | SD height (m) | Volume per ha ($m^3$) | AGB (t/ha) | AGC (tC/ha) | Margalef index** | Disturbance |
|---|---|---|---|---|---|---|---|---|---|---|---|---|---|---|---|---|---|---|
| 1 | Humid | Kisarawe | Degraded forest, shrubs and emergent trees | 39° 5' 51.6" E | 6° 53' 36.9" S | 55 | 14 | 14 | 12.1 | 3.8 | 6 | 8.1 | 2.7 | 23 | 13 | 7 | 2.27 | Fire |
| 2 | Humid | Kisarawe | Lowland forest | 39° 4' 37.7" E | 6° 54' 2.1" S | 100 | 12 | 12 | 33.2 | 23.0 | 38 | 20.8 | 12.6 | 651 | 377 | 189 | 0.40 | No damage |
| 3 | Humid | Kisarawe | Degraded forest, shrubs and emergent trees | 39° 6' 1.9" E | 6° 52' 52.0" S | 25 | 12 | 3 | 6.9 | 2.0 | 2 | 4.6 | 1.4 | 4 | 2 | 1 | 1.21 | Wind and clear felling |
| 4 | Humid | Kisarawe | Lowland forest | 39° 5' 20.6" E | 6° 54' 39.0" S | 95 | 21 | 21 | 20.9 | 7.4 | 26 | 15.5 | 7.1 | 234 | 136 | 68 | 0.66 | Flood Illegal cutting |
| 5 | Humid | Kisarawe | Bushland dense | 39° 5' 14.0" E | 6° 54' 0.7" S | 100 | 15 | 0 | 5.9 | 0.7 | 7 | 3.9 | 0.4 | 13 | 8 | 4 | 0.62 | No damage |
| 6 | Humid | Kisarawe | Degraded forest, shrubs and emergent trees | 39° 4' 7.6" E | 6° 53' 54.6" S | 40 | 12 | 6 | 7.6 | 2.4 | 2 | 4.7 | 1.0 | 5 | 3 | 1 | 0.40 | Grazing |
| 7 | Humid | Kisarawe | Clearing in forest* | 39° 4' 23.6" E | 6° 53' 37.2" S | 100 | 7 | 6 | 21.4 | 11.7 | 11 | 17.1 | 7.8 | 111 | 65 | 32 | 1.03 | Clear felling and charcoal production |
| 8 | Humid | Kisarawe | Clearing in forest* | 39° 4' 18.7" E | 6° 53' 19.7" S | 100 | 9 | 4 | 28.1 | 14.7 | 20 | 18.7 | 6.8 | 234 | 136 | 68 | 1.82 | Clear felling, selective cutting |
| 9 | Dry | Mtera | Woodland closed | 35° 57' 12.9" E | 7° 4' 9.8" S | 50 | 9 | 8 | 21.5 | 1.7 | 28 | 6.8 | 1.7 | 115 | 58 | 29 | 2.17 | Grazing |
| 10 | Dry | Mtera | Woodland open | 36° 0' 30.7" E | 7° 5' 32.6" S | 55 | 18 | 8 | 8.4 | 4.2 | 9 | 4.4 | 1.1 | 24 | 12 | 6 | 1.70 | Selective cutting |
| 11 | Miombo | Itigi | Woodland closed | 34° 43' 26.1" E | 5° 45' 43.4" S | 95 | 32 | 25 | 10.6 | 4.5 | 16 | 6.4 | 1.5 | 53 | 27 | 13 | 2.31 | No damage |
| 12 | Miombo | Itigi | Woodland open | 34° 19' 23.5" E | 5° 48' 40.6" S | 60 | 17 | 8 | 20.4 | 17.7 | 37 | 7.0 | 3.6 | 204 | 102 | 51 | 1.80 | No damage |
| 13 | Semi-humid | Ikiwiri | Lowland forest | 39° 2' 17.8" E | 8° 7' 52.3" S | 100 | 5 | 5 | 28.7 | 26.4 | 32 | 20.6 | 6.2 | 326 | 163 | 82 | 1.86 | No damage |
| 14 | Semi-humid | Ikiwiri | Clearing in woodland | 39° 2' 19.1" E | 8° 7' 51.5" S | 40 | 2 | 0 | 7.1 | 2.3 | 1 | 4.0 | 0.0 | 2 | 1 | 1 | 0.00 | Tree cutting |
| 15 | Semi-humid | Ikiwiri | Woodland closed | 39° 1' 41.9" E | 8° 7' 42.2" S | 50 | 12 | 10 | 20.7 | 14.7 | 24 | 6.9 | 3.2 | 113 | 56 | 28 | 2.82 | No damage |
| 16 | Semi-humid | Ikiwiri | Woodland open | 39° 2' 37.8" E | 8° 6' 29.4" S | 40 | 3 | 3 | 28.3 | 2.9 | 8 | 14.0 | 1.4 | 57 | 29 | 14 | 0.91 | Grazing |
| 17 | Semi-humid | Ikiwiri | Woodland open | 39° 2' 10.0" E | 8° 6' 24.0" S | 30 | 5 | 5 | 25.5 | 9.3 | 9 | 9.6 | 0.0 | 47 | 23 | 12 | 0.62 | |
| 18 | Humid | Kisarawe | Lowland forest | 39° 3' 31.0" E | 6° 55' 34.9" S | 100 | 17 | 17 | 28.6 | 19.7 | 49 | 23.3 | 12.8 | 840 | 487 | 244 | 1.41 | No damage |
| 19 | Humid | Kisarawe | Bushland open with emergent trees | 39° 3' 26.1" E | 6° 55' 52.2" S | 100 | 6 | 0 | 7.0 | 2.0 | 2 | 4.0 | 2.0 | 4 | 2 | 1 | | |
| 20 | Humid | Kisarawe | Degraded forest, shrubs and emergent trees | 39° 2' 53.7" E | 6° 56' 8.4" S | 90 | 5 | 5 | 23.0 | 23.6 | 12 | 5.5 | 8.7 | 137 | 79 | 40 | 1.86 | Damage unknown |
| 21 | Humid | Kisarawe | Lowland forest | 39° 4' 59.6" E | 6° 55' 13.3" S | 100 | 20 | 20 | 25.6 | 17.7 | 39 | 17.2 | 11.8 | 570 | 331 | 165 | | |
| 22 | Humid | Kisarawe | Degraded forest, shrubs and emergent trees | 39° 5' 6.6" E | 6° 55' 19.3" S | 90 | 20 | 5 | 10.5 | 5.4 | 7 | 6.8 | 3.2 | 32 | 18 | 9 | | |
| 23 | Humid | Kisarawe | Degraded forest, shrubs and emergent trees | 39° 4' 58.3" E | 6° 54' 53.6" S | 95 | 12 | 4 | 10.3 | 4.8 | 6 | 5.4 | 2.6 | 21 | 12 | 6 | | |

*Plots n°7 and n°8 values were simulated on the basis of the stumps. In plot n°8 3 out of 9 trees were still present. ** Only the biodiversity index which gave us better results, Margalef index, is shown in the table.

### 5.3.2 Tree distribution

With the location of the trees we created maps of tree distribution for each plot in ArcMap, where each tree is represented by a circle, which size is proportional to its DBH, and is accompanied by its species, height and DBH data. Figure 20 shows the example for plot n°10.

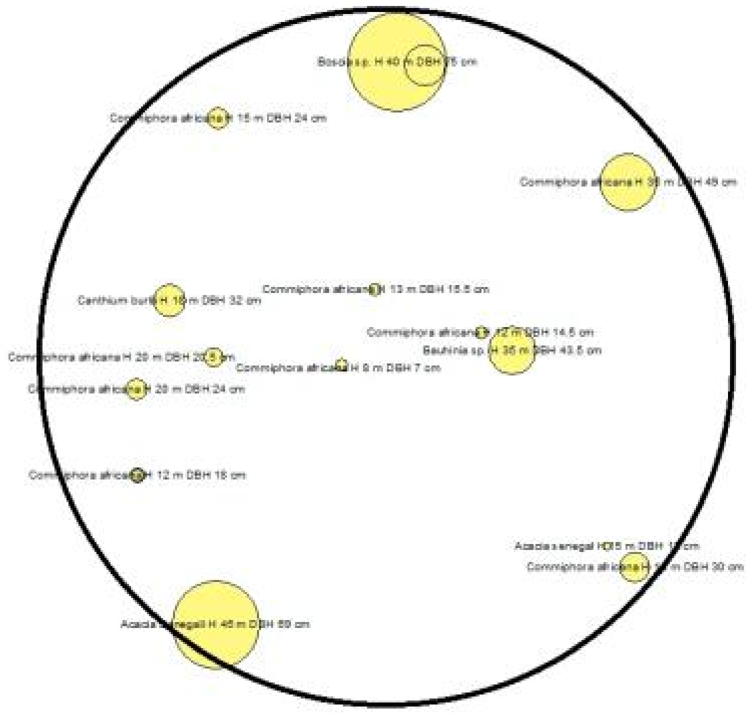


Figure 20: Example of tree distribution map for plot n°10 (dry forest). Every circle represents a tree which DBH is proportional to the size of the circle.

These maps were overlaid on the very high resolution satellite image to analyse the spatial relation with the crown cover as seen in the image. This relation was found weak due to the GPS accuracy and the crowns overlapping in the humid forest.

### 5.3.1 Biome biodiversity indices

The distribution of the species changes by biome. From the humid to the semi-humid and dry there is a dominance of fewer species of the 50% of the total number of tress (Figure 21, Figure 22 and Figure 23).

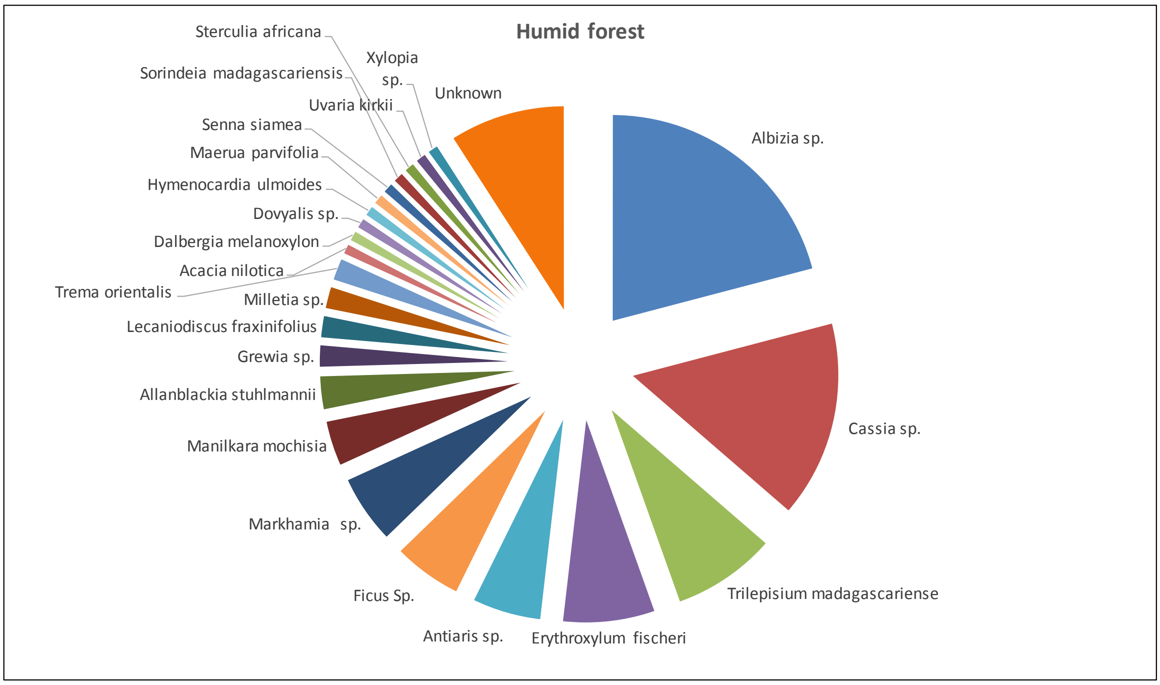


Figure 21: Species distribution within plots sampled in the humid forest.

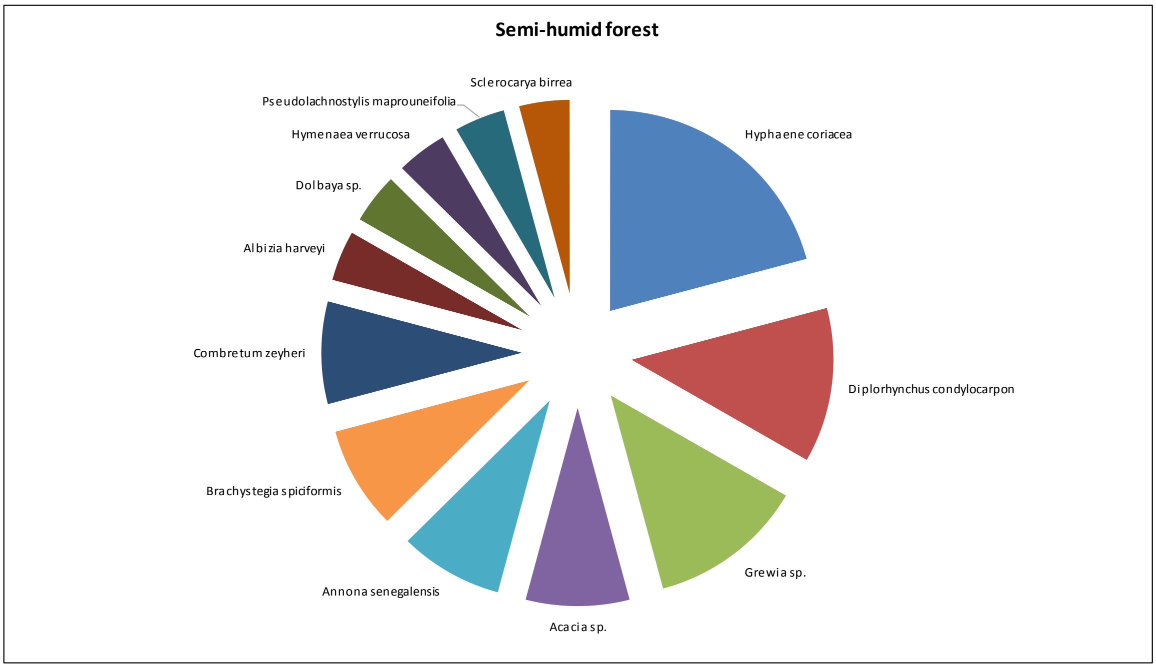


Figure 22: Species distribution within plots sampled in the semi-humid forest.

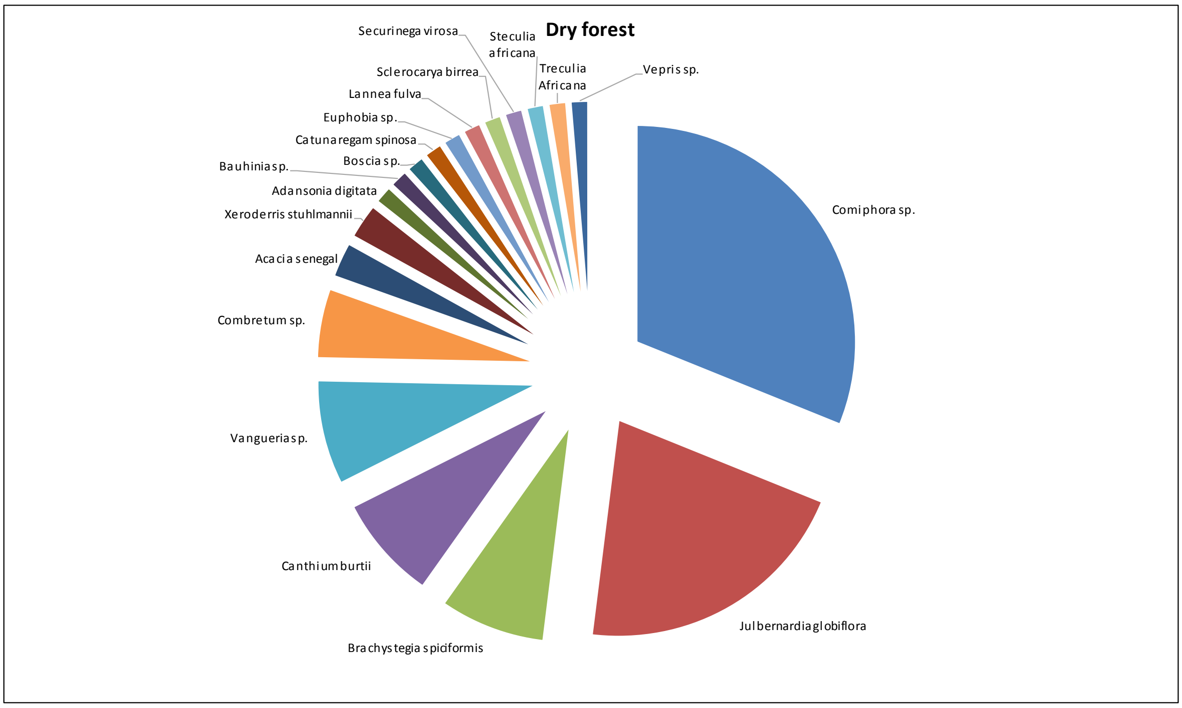


Figure 23: Species distribution within plots sampled in the dry and Miombo forests.

Biodiversity indices were calculated also at biome level, so that changes in biodiversity due to degradation at country level could be monitored in relation to the type of forest (Table 9). The results are just an indication as there are not enough plots to characterize the biome's biodiversity. The humid forest had the highest values, followed by the dry forest. These values can also be affected by the fact that the species were recorded by different persons with different level of experience in each of the three biomes. In the dry forest all the species were identified, while in the humid and semi-humid forests 9.2% and 11% of the trees respectively were not recognised. In these cases, all the unknown trees were grouped in a same class, which decreased the biodiversity values.

Table 9: Biodiversity by biome.

| | N° trees | N° species | Margalef index | Shannon index |
|---|---|---|---|---|
| **Humid forest** | 109 | 23 | 5.11 | 1.15 |
| **Dry forest** | 77 | 19 | 4.14 | 0.97 |
| **Semi-humid forest** | 24 | 12 | 3.33 | 0.94 |

# 6. Vegetation and forest maps production

## 6.1 Vegetation map

A basic classification vegetation map with a minimum mapping unit of 0.5 ha (see segmentation in section *3.3 Plot selection*) was created with the support of the waypoints, photos, vegetation type and undergrowth data from the field survey and visual interpretation of the satellite image (Figure 25).

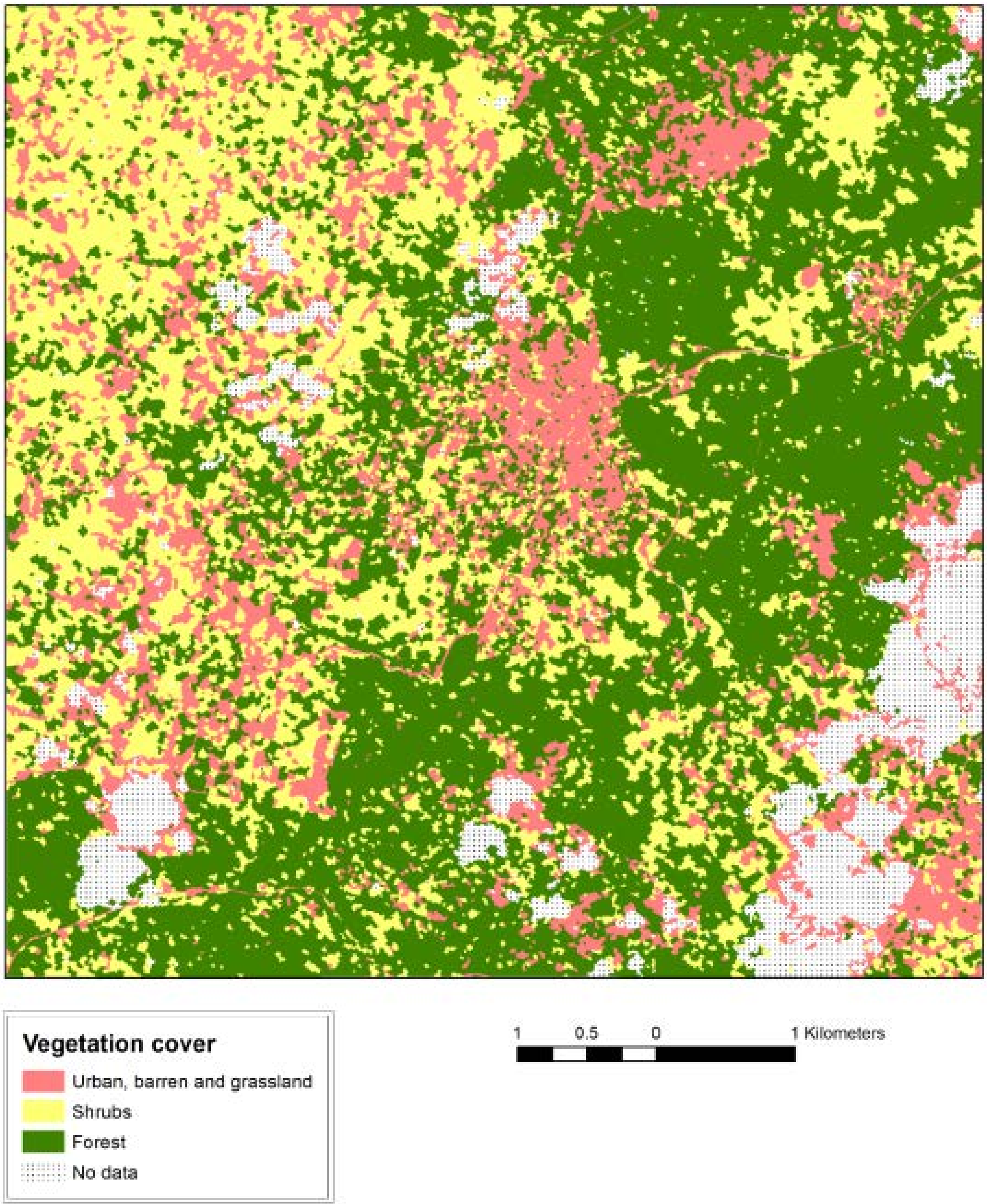


Figure 24: Vegetation map.

## 6.2 Forest maps

Forest areas as identified on the previous vegetation map were classified by biomass related parameters (basal area, height and aboveground biomass) by extrapolating the best regression models obtained from the reflectance and texture information of the image and the field plot data. The changes in these maps are aimed to indicate forest degradation processes.

### 6.2.1 Selection of remote sensing parameters

Image reflectance information is normally used to produce forest classification maps from satellite data. Either indices based on single spectral band information, simple spectral band relations and/or more complex vegetation indices are employed. This type of information have achieved moderate success in tropical and subtropical regions for biomass estimation, where biomass levels are high, forest canopies are closed, with multiple layers, and there is a great diversity of species (Lu 2005). According to some studies (Sarker 2011), texture measures correlate better with biomass than spectral parameters, especially for degraded forests. A combination of both can improve the results (Eckert 2012).

*In a forest degradation process, a homogenization of the image texture and a change in the spectral properties can be related with a loss of the biggest and oldest trees and most valuable species for fuel wood and biodiversity, with the consequent conversion into a single layer of small trees and low diversity of primary species.*

To evaluate the texture of image objects there are two types of texture features: 1) texture features based on analysis of sub-objects, useful for highly textured data, and 2) texture features based on the grey level co-occurrence matrix after Haralick *et al*. (1973). Due to the high level of segmentation of our image, which resulted in small and quite homogeneous objects, we used the texture features after Haralick.

Overlaying the field plots on the segmented image, we selected the image objects containing field plots and extracted a set of pre-selected spectral and textural parameters listed in Table 10 using the image processing eCognition software. Then we examined the potential correlations between these parameters and the field plot parameters.

Table 10: Remote sensing parameters (spectral and textural) extracted from the image objects.

| Remote sensing parameter | Formula / measure |
|---|---|
| **Single band reflectance** | |
| Mean bands 1 to 4 | |
| Standard deviation bands 1 to 4 | |
| **Simple band ratios** | |
| Band 1 to 4 ratios | [Mean band #]/[ SD band #] |
| Standard deviation ratios | [SD band #]/[ SD band #] |
| RVI | NIR/RED |
| GVI | NIR/GREEN |
| GRVI | GREEN/RED |
| **Vegetation indices** | |
| NDVI | $\frac{\text{Mean NIR} - \text{Mean RED}}{\text{Mean NIR} + \text{Mean RED}}$ |

| Remote sensing parameter | Formula / measure |
|---|---|
| EVI | $G * \frac{(NIR - RED)}{(NIR + C1 * RED - C2 * BLUE + L)}$ |
| SAVI | $\frac{NIR - RED}{(NIR + RED + L)} * (1 + L)$ |
| **GLCM texture features** | 1) In all directions, 0°, 45°, 90°, 135°<br>2) For all bands, band 1, band 2, band 3, band 4 |
| Homogeneity | Local homogeneity |
| Contrast | Local variation |
| Dissimilarity | Local contrast |
| Angular 2nd moment | Local homogeneity |
| Entropy | Local variation |
| Mean | Average in terms of GLCM |
| Variance | Dispersion of values around the mean |
| Correlation | Linear dependency of grey levels of neighbouring pixels |

EVI: L is the canopy background adjustment that addresses non-linear differential NIR and red radiant transfer through a canopy; C1 and C2 are the coefficients of the aerosol resistance term, which uses the blue band to correct for aerosol influences in the red band. The coefficients adopted in the MODIS-EVI algorithm are L=1, C1=6, C2=7.5, and G (gain factor) = 2.5.
SAVI: L is the soil brightness correction factor. The value of L varies by the amount or cover of green vegetation: in very high vegetated regions L=0 and in areas with no green vegetation L=1. Generally, an L=0.5 works well in most situations and is the default used value. When L=0, then SAVI = NDVI.

#### *6.2.1.1 Vegetation indices*

The **EVI** (Enhance Vegetation Index) has proved to be sensitive to canopy variations in the tropics. It is an 'optimized' index designed to enhance the vegetation signal in regions with high biomass and improve vegetation monitoring through a decoupling of the canopy background signal and a reduction in atmosphere influences. Whereas the **NDVI** (Normalized Difference Vegetation Index) is chlorophyll sensitive, the EVI is more responsive to canopy structural variations, including leaf area index (LAI), canopy type, plant physiognomy and canopy architecture. The two indices complement each other in global vegetation studies and improve the detection of vegetation changes and extraction of canopy biophysical parameters (Solano 2010).

In areas where vegetation cover is low (*i.e.* <40%) and the soil surface is exposed, the reflectance of light in the red and near infrared spectrum can influence the vegetation index values. This is especially problematic when comparisons are being made across different soil types that may reflect different amounts of light in the red and near infrared wavelengths (*i.e.* soils with different brightness values). The **SAVI** (Soil Adjusted Vegetation Index) was developed as a modification of the NDVI to correct for the influence of soil brightness when vegetation cover is low. The SAVI is structured similar to the NDVI but with the addition of a 'soil brightness correction factor' (Huete 1988).

The use of the both types of indices can improve vegetation classification and vegetation change monitoring in large scale studies which include diverse biomes and vegetation conditions (*e.g.* EVI useful for the non-degraded and humid areas and SAVI for the degraded or dry areas).

#### *6.2.1.2 Haralick texture features*

The grey level co-occurrence matrix (GLCM), is a tabulation of how often different combinations of pixel grey levels occur in an image object. A different co-occurrence matrix exists for each spatial relationship. The feature depends on the direction of concern (all directions or 0°, 45°, 90° and 135° directions) and the spectral bands taken into account (all or each one of the spectral bands).

We produced eight types of Haralick features, which measure similar but varying aspects of texture, called GLCM Homogeneity, Contrast, Dissimilarity, Angular 2nd Moment, Entropy, Mean, Standard deviation and Correlation. There are over 100 textural parameters based on Haralick that can be produced and many of these are highly inter-correlated. In a first step, we remove the duplicate information by running a cross correlation analysis between these parameters.

### 6.2.2 Correlations analysis

The correlations between the field parameters (Table 7) and the remote sensing parameters (Table 8) were examined. Firstly, scatter plots between both set of parameters (one-to one) were depicted to analyse their relationships in order to select the appropriate correlation coefficient. The relationships were relatively linear and so the Pearson's product moment was selected. However, the number of plots to analyse was not large enough to assume a normal distribution, therefore the results cannot be considered significant but rather indicative.

It was found that the average DBH correlated the best with the remote sensing data. As shown in the literature (Feldpausch *et al.* 2011) and in our results (section *5.3.2 Allometric equations*), height is highly related to DBH (in our field data r=0.97), hence, average height also correlated well. Basal area is a derived measure from DBH, therefore it also correlated well. The derived measures of DBH and height, *i.e.* volume and biomass, were worse correlated. Also the variations of DBH and height showed good correlations. However, average canopy cover had a maximum correlation of -0.62, and trees and woody species density maximum correlations of -0.52 and -0.31 respectively. The correlation matrix comparing all the parameters can be found in Annex figure 2 and 3.

The remote sensing parameters that explained most of the variation in the field measurements in general were the ratio of the standard deviations of the NIR and the Red bands (SD NIR/SD Red, a kind of vegetation index), the texture features of local homogeneity 'GLCM Angular 2nd moment' and 'GLCM Homogeneity in all directions', and the texture feature of local variation 'GLCM Entropy'. Table 11 shows the Pearson coefficients from the best correlations between these parameters and the field parameters.

Table 11: Best Pearson correlation coefficients (r) between the remote sensing parameters and the field parameters with the significance level (p-value).

| | Average DBH | | Average height | | Basal area | | AGB | | Volume | | SD DBH | | SD Height | |
|---|---|---|---|---|---|---|---|---|---|---|---|---|---|---|
| | r | p-value | r | p-value | r | p-value | r | p-value | r | p-value | r | p-value | r | p-value |
| **SD NIR/SD Red** | 0.92 | 1.83E-5 | 0.88 | 7.55E-5 | 0.79 | 4.72E-3 | 0.73 | 1.83E-5 | 0.73 | 4.47E-3 | 0.77 | 1.86E-3 | 0.73 | 4.71E-3 |
| **GLCM Angular 2nd moment** | 0.91 | 3.45E-5 | 0.88 | 1.10E-4 | 0.74 | 6.71E-3 | 0.71 | 3.45E-5 | 0.71 | 6.43E-3 | 0.69 | 9.50E-3 | 0.65 | 1.58E-2 |
| **GLCM Homogeneity all directions** | 0.90 | 3.06E-5 | 0.89 | 4.5E-05 | 0.70 | 1.22E-2 | 0.66 | 3.06E-5 | 0.66 | 1.39E-2 | 0.68 | 1.04E-2 | 0.62 | 2.46E-2 |
| **GLCM Entropy** | -0.9 | 9.67E-6 | -0.87 | 8.79E-5 | -0.72 | 4.07E-3 | -0.69 | 9.67E-6 | -0.69 | 8.63E-3 | -0.70 | 7.14E-3 | -0.63 | 1.97E-2 |

### 6.2.3 Multiple regressions

The variability in the field measurements that could be explained by the remote sensing parameters was estimated by multiple regressions in the statistical software R (R Core Team 2012).

Some of the remote sensing parameters were highly correlated with each other. We used correlation matrixes to identify the most relevant ones for the regression models and remove the redundant data. As a first approach, we grouped the parameters which were highly inter-correlated and from each group we chose the most relevant one for predicting a particular field measurement. As a second approach, we filtered out the parameters which resulted with more than $r^2 > 0.70$ of inter-correlation. The inclusion of the second set of parameters gave us better fitting models. These set of parameters included the standard deviation of band 2, GLCM Angular 2nd moment, GLCM Homogeneity at 45°, NDVI, GLCM Variation and mean of band 4 (Annex figure 4).

Multiple regression models were calculated for only those field parameters which showed the best correlations, *i.e.* DBH, tree height, basal area and biomass. To select the 'best' model, we used the Akaike Information Criterion (AIC), which is a measure of the relative quality of a statistical model for a given data set. It is based on the trade-off between the fit of the model and the complexity of the model. That is, it rewards the goodness of fit, but includes a penalty which is an increasing function of the number of independently adjusted parameters, so it discourages over-fitting. It is calculated with the following function: $AIC = 2k - 2\ln(L)$, where k is the number of parameters in the model and L the maximum value of the likelihood function of the model (Akaike H. 1974). Table 12 shows the best models for each of the field parameters (linear for DBH and height and exponential for basal area and biomass).

Table 12: Best fitting equations for the multiple regressions models for DHB, height, basal area and biomass with the remote sensing parameters.

| | Best fitting equation | $R^2$ | p-value |
|---|---|---|---|
| DBH | 41.16 +230300 GLCM Angular2 -0.032 Mean 4 -0.63 SD2 | 0.95 | 5.76e-7 |
| Height | 76.56 +186000 GLCM Angular2 -0.026 Mean4 -0.6 SD2-53.47 NDVI | 0.93 | 3.77e-5 |
| Basal Area | EXP(-111.8 +37.81 GLCM H45 +2.046 GLCM SD2 -0.0077 Mean4 +35.74 NDVI) | 0.86 | 3.00e-4 |
| Biomass | EXP(-179+ 70.5 GLCM H45 +3.201 GLCM SD2 -0.012 Mean4 +59.01 NDVI) | 0.84 | 5.56e-4 |

To check the validity of the models, scatter plots were produced between the field measured data and the modelled results (Annex Table 5). The points fitted well with the regression line, but were not equally distributed; there are missing points for DBH in the 15-20 cm range and for height in the 10-15 m range.

### 6.2.4 Calibration of the satellite image

The equations derived from the multiple regressions were then applied to all the forest polygons from the vegetation map to produce maps of tree height, basal area and biomass. Previously, the four remote sensing parameters included in the models had to be retrieved from all the polygons. The regressions are not fully robust, in that the variance of the models estimations can be high. Therefore we visually reviewed the maps to remove obvious misclassifications.

#### 6.2.4.1 Map of tree height

After masking non-woody areas (grass, barren and urban) and no-data (clouds and cloud shadow) the height parameter was used to classify the polygons into shrubs (<5 m) and trees (>5 m). Within these two categories, we further divide the polygons into two classes of shrubs (<2 m and >2 m) and three of tree height (5-10 m, 10-15 m and >15m) (Figure 26).

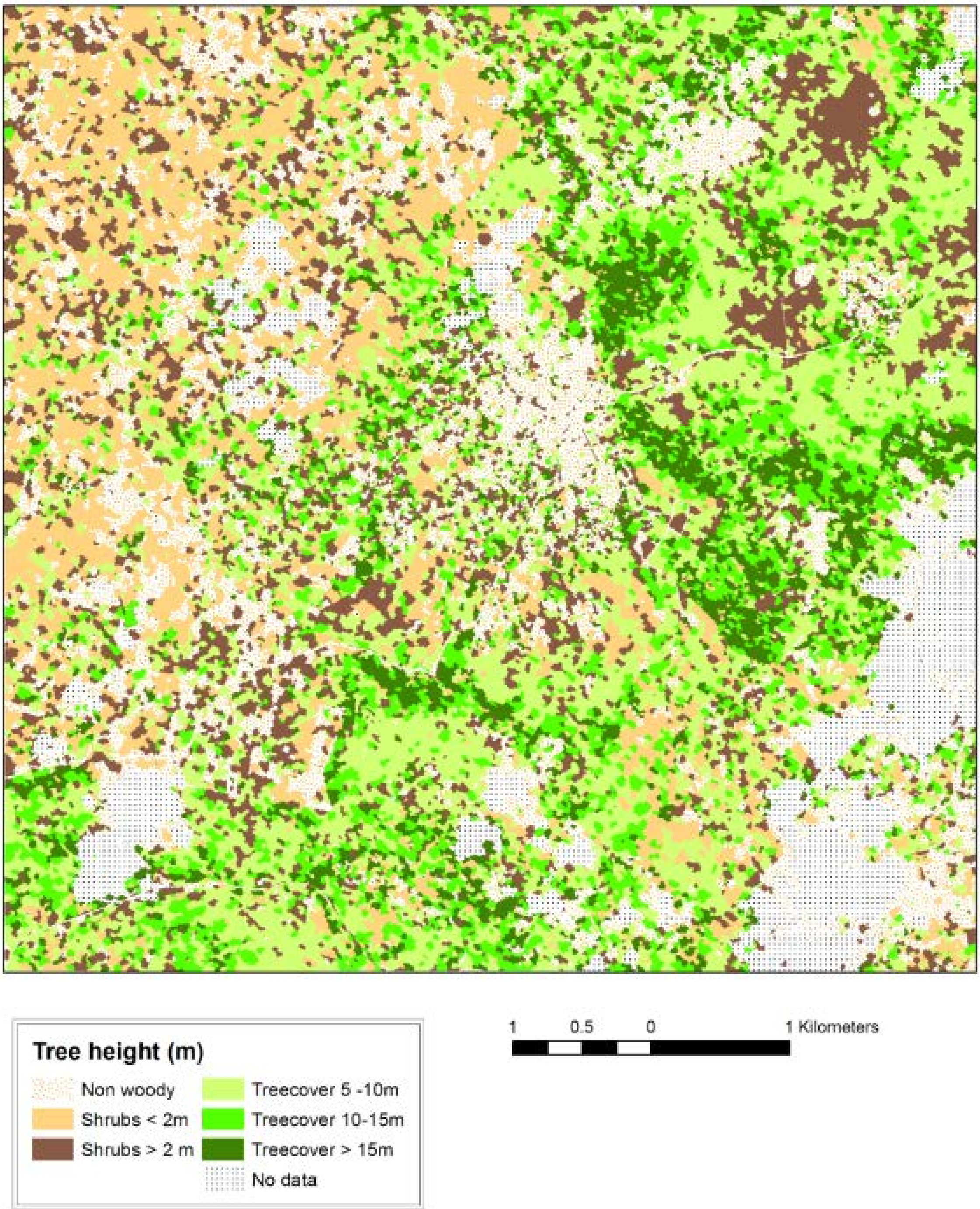


Figure 25: Map of tree height

#### 6.2.4.2 Map of basal area

A map of basal area was produced, rather than a map of DBH, as it is closely related to forest management. Within the forest class we map four classes of basal area (Figure 26).

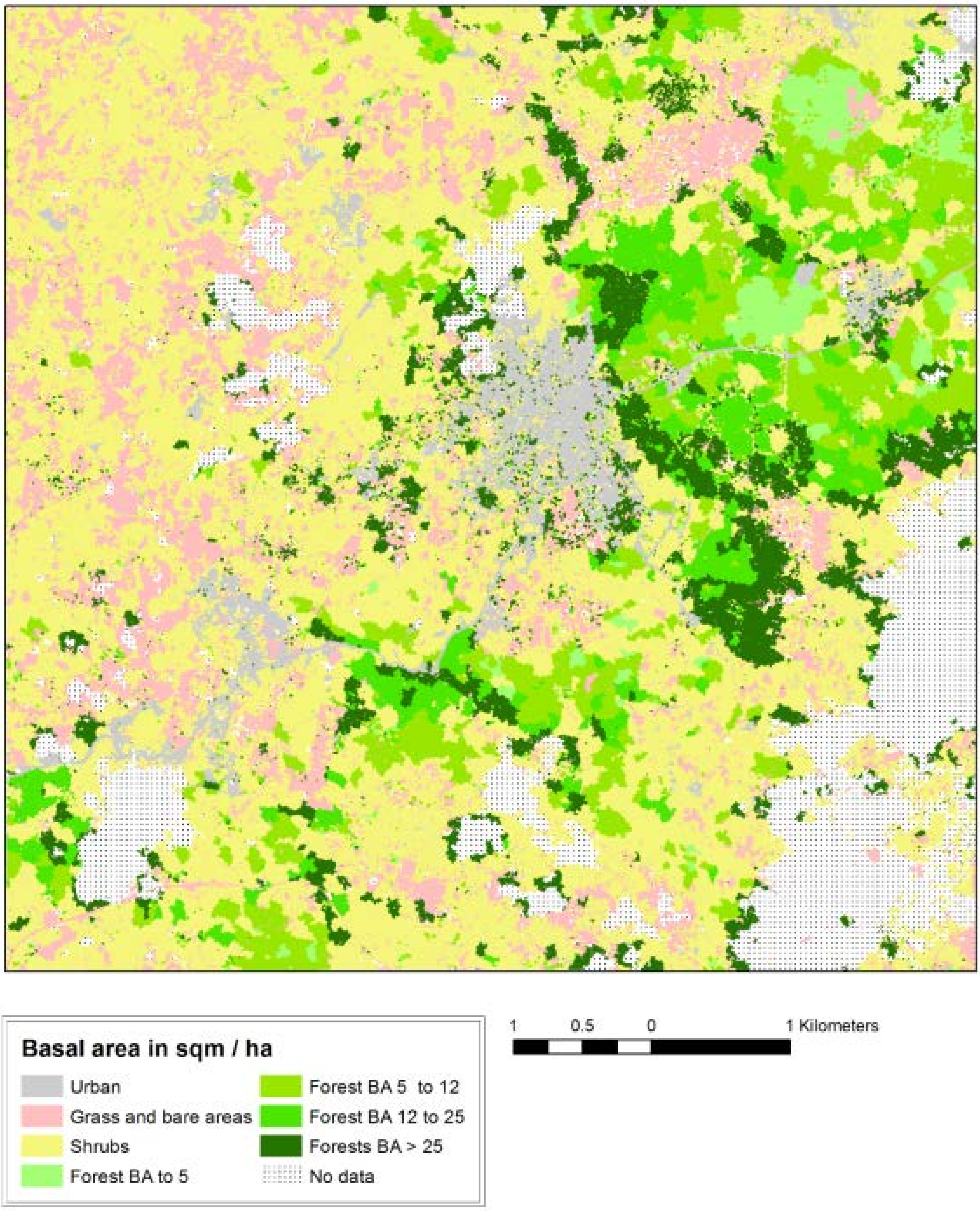


Figure 26: Map of basal area (BA).

#### 6.2.4.3 *Map of aboveground biomass*

Finally a map of aboveground biomass was produced for the study area. Note that there is a low representation of the highest biomass class. This is because few areas of pristine forest remain, mainly on steep inclines, with maximum biomass values of 250 tC/ha. Is in line with other studies, such as Lewis *et al.* 2013, where closed-canopy tropical forest across 12 African countries had on average 197tC/ha. In these case however, most of the samples were located in Central Africa.

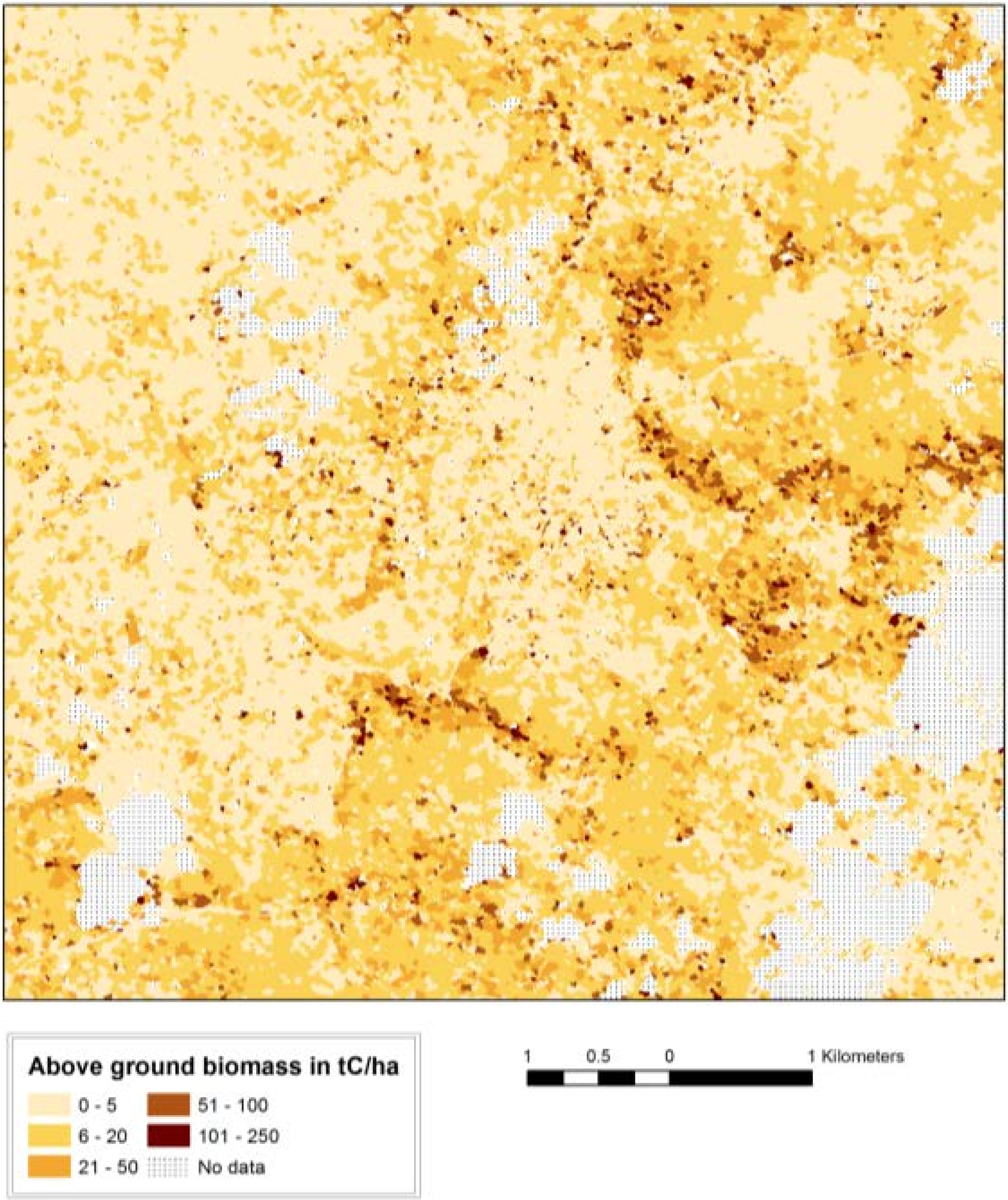


Figure 27: Map of aboveground biomass in tC per hectare.

## 6.3 Validation

Validation data were collected in a short field mission of two days. To obtain a rapid validation data set, rather than repeating the full field data collection, which has considerable time requirements, only the average canopy height was measured at 31 random locations across the primary field site in Kisarawe (Figure 28). Ideally, average tree DBH and average tree height should have been calculated to validate the maps of tree basal area, tree cover height and aboveground biomass, but these parameters require a lot of time to take many single tree measurements. As an alternative, the average canopy height was estimated once per location from the outside of the plot with the laser rangefinder. Highly significance inter-correlation between mean tree height and estimated canopy height was found in a data analysis of 50 plots between 0.012-0.25 ha along the coast of Tanzania (covering a total area of over 4.4 ha), primary used to produce transect diagrams (Lowe A.J. and Clarke G.P., in Burgess 2000). There were some difficulties to measure the average canopy height, for example when forests had multiple tree layers or the centre of the crown was obscured. Nevertheless, the estimated average canopy height data were used to assess the general validity of the map production approach.

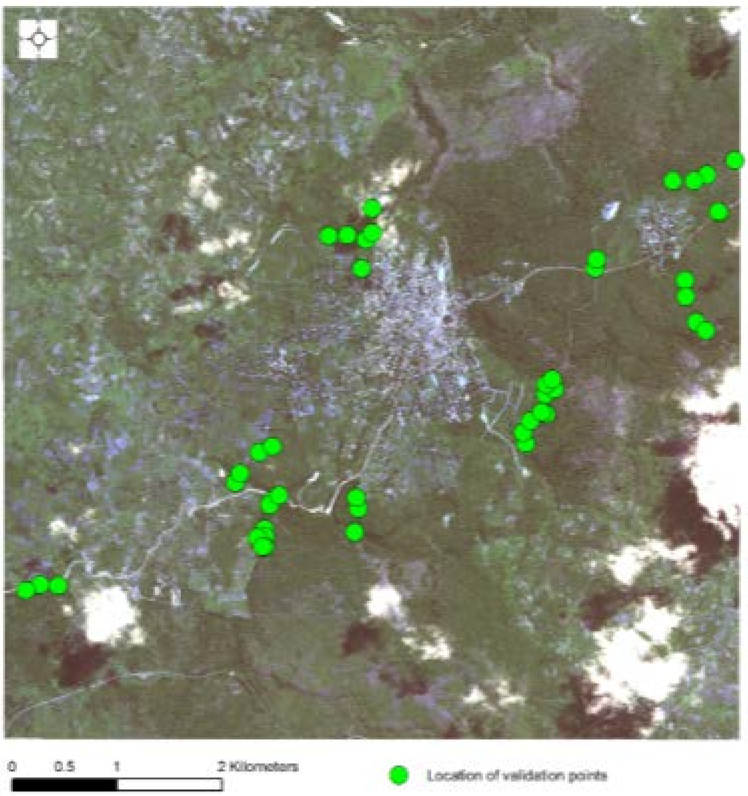


Figure 28: Location of the validation data on average canopy height.

For 31 validation locations, the average tree height was calculated from the model of tree height (Table 12). Other validation locations were not used because on the image either they were in mixed cover polygons (*e.g.* trees and grass or stands of different height), or had atmospheric effects (*e.g.* fine haze or shadow), that had a strong influence on the remote sensing parameters extracted.

A confusion matrix was made for the correspondence of measured average canopy height (validation) and modelled average tree height (map) (Table 13), using the four tree cover height classes (≤5 m, >5 and ≤10m, >10 and ≤15m and >15m). It resulted that 55% of the points had been correctly classified, 6.4% overestimated (error of commission) and 39% underestimated (error of omission) in the map regarding the validation data. The model tended to underestimate canopy height from class 5-10 m onwards.

Table 13: Contingency table between the field measurements on canopy height (validation) and the modelled results on tree cover height (map).

| | Validation | | | | | |
|---|---|---|---|---|---|---|
| Map | **n=31** | **≤5 m** | **5-10 m** | **10-15 m** | **>15 m** | **Sum** |
| | **≤5 m** | 8 | 3 | 0 | 1 | 12 |
| | **5-10 m** | 2 | 5 | 4 | 1 | 12 |
| | **10-15 m** | 0 | 0 | 1 | 3 | 4 |
| | **>15** | 0 | 0 | 0 | 3 | 3 |
| | **Sum** | 10 | 8 | 5 | 8 | 31 |

The possible errors in the classification could also be due to the way the validation data were obtained. Measuring the average canopy height from the outside of the plot can lead to an overestimation of the real average tree height, especially when forests reach certain height (>5 m) and form several layers. In these cases, if the canopy is too close, the low layers are covered by the top layers and not taken into account in the estimation. On the other hand, these shorter trees were measured in the field survey, decreasing the tree height average of the plots. This overestimation was also observed in the previously mentioned study in Burgess 2000 (see Annex figure 6). Also, obtaining an 'average' canopy height is problematic when the mapping unit is large, as there may be a large variance within the land units.

# 7. Lessons learnt, conclusions and limitations

There are a number of points in the planning, preparation and execution of the field exercise that we found needed to be emphasised and in some cases improved.

### 7.1 Field survey planning

Bad planning can lead to an excessive amount of time lost either when travelling to the sites or reaching the plots, or by measuring on the wrong locations.

#### 7.1.1 Route planning

Good route planning for the site visits is essential to avoid time loss. GIS layers were at times found to be unreliable (*e.g.* a road in our road layer was in fact a railway, see Figure 29). Google Earth, which was extremely useful for mission planning and navigation, occasionally had some cases in miss location. Also roads can be under renewal, resulting in frequent detours and obstruction by construction crews and machinery. Therefore it is advisable to purchase the most updated road map in the country and ask for information *in situ* before setting out.

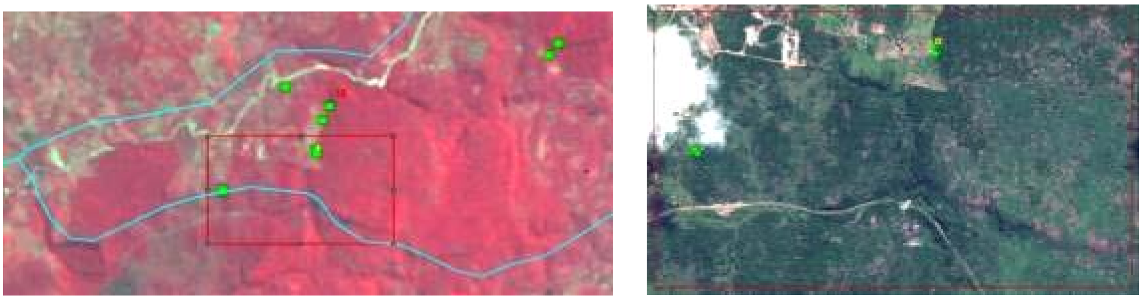

Figure 29: Road GIS layer (left) and Google Earth image (right), with the railway.

#### 7.1.2 Plot selection

The final selection of the plots did not always correspond to the location initially chosen due to several reasons. The first was the accessibility to the plots. In the study area primary forest is remaining mainly in hillsides, which were at times difficult to reach or on very steep slopes. Local topographic maps can be very helpful for evaluating the accessibility to the plots beforehand. Secondly, some areas had undergone land cover changes by the time of the field work. It is important to check the orthomaps in the field for avoiding measuring plots with major changes since the image acquisition. Thirdly, it is important to ensure that plots fall into cloud free areas on the satellite imagery, which can be already done in the preliminary selection of the plots.

Travelling through dense undergrowth, passing water courses and having to climb excessive slopes, all reduce time spent in making measurement. Plots should therefore be selected with easy access. However, care is needed to avoid oversampling in plots more likely to be affected by anthropogenic impact.

To ensure that there is an adequate distribution of field data, one needs to ensure that a good cross-section of the required variable is sampled (*e.g.* biomass, tree height). Pre-analysis of plot results during the mission can help to re-program subsequent plot visits. It is advisable to be flexible: if data already collected are not equally distributed in the different strata of vegetation types or the study variable, new plots can be sought.

## 7.2 Data collection

Before embarking on mission, it is important to test all equipment and to carry out at least one trial plot measurement protocol.

### 7.2.1 GPS records

At least two GPS were found to be essential for the mission, one at high sample rate for plot location and another at a lower sample rate for route tracking. A third one would be advisable in case there is a local topographic datum for data integration with national field surveys or cartographic products. Better GPS location of waypoints can be obtained by averaging readings over a period of time. Once acquired, the waypoint position accuracy can be improved by selecting the waypoint on the device and using ‘Average Location’.

The GARMIN GPSMap 60CSx used in the field survey has at best 6 m accuracy, so fine positioning of the plots on the very high spatial resolution imagery is not always easy. It is advisable to mark reference points on the orthomaps and on the GPS for later orthorectifying the GPS points on the image. Also, a high sample rate for tracking is required for a good geolocation of the points (1 second was used in the study), however care is needed to ensure that the memory card does not fill up.

### 7.2.2 Plot measurements

It is important to define a measurement and data recording protocol, and meticulously adhere to it, unless amendments are required, otherwise required parameters are difficult to retrieve from data obtained by different approaches.

Of the original field measurements planned, crown measurements of individual trees was found difficult to obtain, due to the canopy structure obscuring clear line of sight for the laser rangefinder. Therefore, the aboveground biomass estimation was done based on the bole volume as single variable, which has been proved to give good results in previous studies.

Also the geolocation accuracy of the plot centre and tree locations on the image was problematic. First, the GPS measured with +/- 3 m accuracy, which for a satellite image of 0.46 m spatial resolution can mean a considerable displacement. Second, in closed forest where there was significant undergrowth, it was difficult to find a line of sight from the centre of the plot to the tree stands (see Figure 3132 in *section 7.3 Image interpretation*).

Whether collected digitally, or in written form, all data must be reviewed at the end of the day’s field visit. Any errors or omissions can be quickly rectified at this point.

### 7.2.3 Field equipment

The field survey was executed using basic, readily available and inexpensive tools (standard GPS, spherical densitometer, digital camera and paper data forms), so all forest services can carry out a similar exercise. However more expensive and sophisticated instruments exist and should be kept in mind. For example, more accurate GPS models (decimetre accuracy), spherical photograph for measuring canopy cover or compact field computers (*e.g.* the Juno SB handheld, Trimble 2014) integrating many functionalities, including high sensitivity GPS receiver, photo camera, data collection facilities, GIS and satellite imagery software (such as ArcGIS Mobile) and real-time or post-processing position corrections for higher accuracy. The investment in such equipment remains relatively high but leads to greater productivity, allowing more data to be collected in less time and with higher fidelity.

The accurate position of measurements made in the field on the satellite imagery is essential if they are to be correlated with remote sensing parameters. The use of decimetre accuracy GPS models should especially be considered if 'tree precision' accuracy (*i.e.* the capacity to identify an individual tree on an image) is required.

The laser rangefinder was the most expensive and sophisticated instrument used in the field survey. However the measurements done with it could have been done with other basic and inexpensive tools (*e.g.* tree height with a hypsometer). In fact, it was useful in open forests, but in closed forests it was difficult to find a line of sight both for tree location and height (Figure 3031). In these cases the height of the trees was estimated visually, averaging the estimation of three persons of the crew, which in previous tests resulted to be very similar to the measure taken with the laser rangefinder.


Figure 30: Tree height and position measurement with the laser rangefinder in the dry (left) and humid (right) forests. In the latter, the undergrowth impedes the laser from hitting the trunk and the top of the crown.

### 7.2.4 Validation data

The rapid validation exercise for the model of tree height (section *6.3 Validation*) can be improved. The field plots were pre-selected inside homogeneous polygons, while the validation data were measured on random locations. Hence the model prediction of average tree height reflected the full land units, whereas the validation data on average canopy height a specific point within the unit, and therefore some of these were at odds with the model prediction. For this reason, a number of the validation points collected which fell in land units with highly contrasting tree heights were not considered, neither those located in polygons affected by atmospheric effects, such as haze or shadow. Therefore, to render the validation exercise more efficient the validation points should be equally pre-selected in homogeneous polygons with no atmospheric effects.

## 7.3 Image interpretation

### 7.3.1 Data analysis

When relating image properties to field data, care is needed to take into account possible differences in the time of the image acquisition and the field visit. This often occurs due to the low acquisition rate of satellite images over certain areas or to the high rate of land cover change dynamics in others. We found during the field visit that some plots had been modified since the image acquisition time. In two instances, when the trees had been cut, we overcame this by recreating the initial forest state height, volume and biomass extrapolating measures from the remaining stumps using allometric equations calculated with the rest of the field data.

There was an attempt to analyse the spatial relation of the estimated crown cover from the field measurements with the canopy cover as seen on the satellite image. As the crown diameter was difficult to measure in the field, the crown area was estimated from the DBH with allometric equations from the literature. Then tree crown maps of the plots were recreated in ArcMap and overlaid on the very high resolution satellite image. The relation did not give good results due to crowns overlapping in the humid forest (Figure 31).

Figure 31: Example of estimated tree crown cover map from DBH field measures of plot n°18. Map of estimated tree crown area over the satellite image (left) and picture of the tree DBH measurements (right). The yellow circles represent the crown area of individual trees and the green dots the position of the tree stands.

When one type of field measurement has to be done by different members of the crew during the field survey, care is needed to ensure consistency. We found some inconsistencies in the canopy cover measures taken with the spherical densitometer, due to different approaches in counting the half-filled squares by tree cover. Therefore it is advisable that the crew members are trained together in the use of the instruments.

### 7.3.2 Map production

The field parameters best correlated with the remote sensing parameters were DBH, followed by tree height, basal area and aboveground biomass. From the remote sensing parameters, the ratio of the standard deviations of NIR and Red bands (SD NIR/SD Red) was the best correlated with DBH, basal area, and biomass, closely followed by the texture measure 'GLCM homogeneity in all directions', which was the best correlated with height.

Average canopy cover had a lower correlation with the remote sensing parameters. One of the reasons could be the already mentioned inconsistency between the measurements and that the canopy cover was measured at shoulder height. It is important to understand that whereas the field measurements relate to volumetric quantities (*e.g.* biomass), the remote sensing data are based on top canopy related qualities, *i.e.* what is seen from above, and this can lead to some mismatching. For example, the canopy measurements made at 1.6 m height, may include tree and shrub layers covered by higher layers which are not recorded by the satellite.

The multiple regression models linking the field parameters (DBH, tree height, basal area and biomass) with remote sensing parameters were significantly improved by the addition of texture measures. This is not surprising when using satellite imagery of this high spatial resolution, as the canopy structure, which depends on the tree sizes, is well represented by the image texture.

The multiple regression models only included the NDVI from the possible vegetation indices as one of the explanatory variables. The use of NDVI alone could be enough because all the plots in the study belong to the humid forest domain. The inclusion of the other vegetation indices, EVI and SAVI, could be useful at a country level study, where there are diverse biomes and soil conditions.

The models were constructed with data from polygons with homogeneous texture and reflectance, but then applied to the full segmented image which had also heterogeneous polygons. These had higher variance in tree crown sizes or holes in the canopy, which could affect their correlation of the reflectance, but especially of the textural parameters, with the field data. This suggests that to improve the results, either heterogeneous polygons should be employed in the construction of the models, or a finer MMU should be used in the segmentation of the image. The size of the polygons obtained with a MMU of 0.5 ha could be good for studies with lower spatial resolution satellite images (approximate 5-10 m), but too large for this resolution.

Where as in the field it was difficult to measure canopy cover at the actual canopy height level, this can be directly measured from the image at this fine resolution. For this, a sub-segmentation of the polygons could be used to determine the percentage of canopy cover at the minimum mapping unit.

## 7.4 Conclusions

***Utility of the study***

To monitor forest degradation for the REDD+ programme, we need to monitor changes in the forest canopy cover, and also estimate changes in the forest carbon stock caused by human influences. The utility of very high resolution satellite data for deforestation monitoring has been demonstrated with respect to Landsat data. In this study, forest units were mapped at 0.5 ha, with a series of forest parameters (tree height, basal area and above ground biomass) which can be used in the management and carbon stock reporting of the Pugu Hills forests. These characteristics cannot be mapped with confidence from the widely available Landsat sensor.

This forest mapping approach is based mainly on vegetation structural parameters. Environmental factors affect the vegetation structure in the forest, but human disturbances also have an important influence on it, reducing parameters such as basal area and stem density. For instance, those of our plots where some type of human disturbance was recorded exhibited lower basal area (Table 8). The study of Burgess (2000) suggests that human disturbances have a major influence in the structure of the costal forest of eastern Africa, and moreover that these disturbances remain detectable in the forest structure for many years. Disturbed forests have a low basal area and stem density even after 30-80 years the disturbance took place. Therefore, measurement of structural parameters is a good approach for detecting forest degradation by human disturbances, but changes of these parameters have to be monitored at long time scales.

In addition to this, structural parameters have the advantage that they are detectable and measurable using remote sensing techniques. In satellite imagery of very high spatial resolution, such as the Worldview-2 data, the textural properties of the forest can be well characterised and even tree crowns identified. As tree crown is related to DBH, the volume of the biomass could be directly retrieved using allometric equations. However, in close forests with overlapping tree crowns, only the top layer is recorded by the satellite images. Therefore, we followed an indirect approach, where the reflectance and texture parameters of the image were calibrated to biophysical variables related to forest biomass.

To calibrate the satellite images field survey is necessary, especially in the humid forest. Heavily disturbed forests that have regenerated freely may appear in pristine conditions, but they still retain evidences of such disturbance in the structural parameters. From field measurements we built the biophysical variables (*i.e.* basal area, height, volume and biomass) with general allometric equations grouping all species together. Important variations in volume geometry, wood density and carbon content between and within ecological zones and tree species have been reported in the Sub-Saharan African forest allometric equations (Henry 2011). However according to some authors, grouping all species together and using generalized allometric relationships, stratified by broad forest types or ecological zones, is highly effective for the tropics. This is because DBH alone explains more than 95% of the variation in aboveground carbon stocks in tropical forest, even in highly diverse regions (Brown 2002, Gibbs *et al.* 2007).

***Limitations***

In the field survey only the variables related to aboveground biomass were measured, which is usually the largest carbon pool in the forest and the most directly affected by deforestation and degradation. However, belowground biomass can represent an important portion of the total forest biomass, especially in dry areas. Measuring the biomass of the rooting systems is very costly and time consuming. Fractal geometry can be a good proxy to overcome the problems arising from the sampling of belowground tree biomass (Hairiah et al. 2001). For example, there is an inventory of available root-to-shoot ratios for the entire tropical domain created by the IPCC (2006). Apart from this, soil properties (*e.g.* fertility, compactness and salinization) could complement the study, as they can indicate an early stage of degradation which is not visible in the vegetation structure.

When using single date satellite images for mapping forest structural parameters, values cannot be compared to historical references. This is often unavoidable in the case of high spatial resolution satellite data, which became available only in the recent years (*e.g.* Rapideye satellite was launched in 2009) or which are difficult to find over certain areas (*e.g.* very high spatial resolution Worldview-2 data). For such cases, environmental factors should be taken into account in order to relate low values of basal area, height or biomass to degradation processes induced by human activities. This is because vegetation structure in the forest is also affected by factors such as altitude, water availability and edaphic properties. For example, Burguess (2000) found that areas with groundwater and deep soil had large and well-spaced trees, areas with rocky outcroppings and shallow soil had low trees, and areas in higher altitude (with higher rainfall), tall and large trees and intermediate or low density.

Satellite images of very high spatial resolution have the drawback in that they are difficult to find for certain areas, very expensive and cover small areas. Therefore, it is difficult to cover a full country with such images for national studies, such as in the Tanzania national REDD+ initiative. They can be useful however to calibrate satellite images of lower spatial resolution, but higher acquisition frequency and broader coverage, as the 10 m spatial resolution RapidEye data.

Due to time restrictions the total number of plots measured in the field survey was low. The reduced calibration dataset limited the significance of the correlations between the field measurements and the remote sensing parameters, and the robustness of the models to construct the forest structural maps. Moreover, the lack of sufficient data on species compositions precluded the analysis of the biodiversity indices with field measurements and remote sensing parameters.

When carrying out the field survey it is difficult to avoid an over influence of human activities, as the most accessible areas for sampling are close to roads or paths and therefore more likely to be used for fuel wood collection or charcoal production. However, this is not a main problem in this study, as the field survey was not aim at supporting statistical national studies, but characterising the main forest types as seen on the satellite image.

We found that a more structured approach to validation is needed. An *ad* hoc validation scheme, relying on improvisation in the field results in unreliable data. We found that many of our field measurements (single tree height) did not represent the average tree height in the land unit measured. The validation approach should therefore be reconsidered.

***Future work***

The statistical analysis was done only with the field data from the humid forest, as not enough data from the semi-humid, dry or Miombo forests were collected. Our models could be applied to the other biomes to see if they are appropriate, or new models have to be created. In this case, allometric equations, stratified by broad forest types or ecological zones, should be applied.

With more data on species compositions, appropriate biodiversity indices could be calculated at biome level, so comparisons between structural and species ordinations at country level could be monitored in relation to the type of forest.

The final map is a single date image classification of biomass. However, forest degradation is a temporal process. To discriminate forest degradation the maps should be redone in the future with newer imagery for change monitoring.

As the goal of this work is to improve on the rapid collection of field data, we will review our procedures and include newer technology, GPS and data collection tools.

# 8. References


Achard, F., Beuchle R., Bodart C. *et al.* 2009. Monitoring forest cover at global scale: the JRC approach. *Proceeedings of the 33rd International Symposium on Remote Sensing of Environment (ISRSE), 4-8 May 2009, Stresa,Italy,* p. 1-4.

Achard, F., Beuchle R., Mayaux P. *et al.* 2014. Determination of tropical deforestation rates and related carbon losses from 1990 to 2010. *Global Change Biology,* 20, 2540-2554.

Akaike, H., 1974. A New Look at the statistical model identification. *IEEE Transactions on Automatic Control*,19(6),710-723.

Bodart, C., Brink A., Donnay F. *et al*. 2013. Continental estimates of forest cover and forest cover changes in the dry ecosystems of Africa between 1990 and 2000. *Journal of Biogeography,* 40, 1036-1047.

Brown, S. 1997. Estimating biomass and biomass change of tropical forests: a primer. In FAO Forestry Papers 134, FAO, Rome, Italy, 55 pp.

Brown, S. 2002. Measuring carbon in forests: current status and future challenges. *Environmental Pollution*, 116, 363–372.

Burgess, N.D. & Clarke G.P. (Eds.) 2000. Coastal Forest of Eastern Africa. IUCN, Gland, Switzerland and Cambridge, UK, 443 pp.

Chamshama, S.A.O., Mugasha A.G., Zahabu, E. 2004. Stand biomass and volume estimation for Miombo Woodlands at Kitulangalo, Morogoro, Tanzania. *South African Forestry Journal*, 200, 59-70.

Condit, R. 1998. Tropical forest census plots. Springer-Verlag, Berlin, Germany, pp.211.

EC, 2013. EU to support Tanzania in protecting its forest. Press release, Dar es Salaam 27th March 2013. Retrieved on 1 may 2013 from:
http://eeas.europa.eu/delegations/tanzania/press_corner/all_news/news/2013/press_release-eu_to_support_tanzania_in_protecting_its_forest_cover.pdf

Eckert, S. 2012. Improved forest biomass and carbon estimations using texture measures from WorldView-2 satellite data. *Remote Sensing Open Access*, 4, 810-829.

ERDAS, 2002. ERDAS Field Guide™. Sixth Edition. ERDAS Inc., Atlanta, Georgia.

Eva, H., Carboni S., Achard F. *et al*., 2010. Monitoring forest areas from continental to territorial levels using a sample of medium spatial resolution satellite imagery. *ISPRS Journal of Photogrammetry and Remote Sensing*, 65 (2), 191-197.

FAO, 2007. Definitional issues related to reducing emissions from deforestation in developing countries. (Eds: Schoene D., Killmann W., von Lüpke H., LoycheWilkie M.) Forests and Climate Change Working Paper 5. FAO, Rome, Italy. Retrieved on 11th November 2014 from: http://www.fao.org/docrep/009/j9345e/j9345e00.htm.

FAO, JRC, SDSU and UCL 2009. The 2010 Global Forest Resources Assessment Remote Sensing Survey: an outline of the objectives, data, methods and approach. Forest Resources Assessment Working Paper 155. FAO,Rome, Italy.

Feldpausch, T.R., Banin, L., Phillips, O.L. *et al.* 2011. Height-diameter allometry of tropical forest trees. *Biogeosciences*, 8, 1081–1106.

Gibbs, H.K., Brown, S., Niles, J.O. *et al.* 2007. Monitoring and estimating tropical forest carbon stocks: making REDD a reality. *Environmental Research Letters,* 2, 13.

Hansen, M.C., Potapov P.V., Moore R. *et al.* 2013. High-resolution global maps of 21st-Century forest Cover change. *Science*, 342 (6160), 850-853.

Haralick, R.M., Shanmugam, K., Dinstein I. 1973. Textural Features for Image Classification. *IEEE Transactions on Systems, Man, and Cybernetics*, SMC-3 (6), 610–621.

Henry, M., Picard, N., Trotta, C. *et al.* 2011. Estimating tree biomass of sub-Saharan African forests: a review of available allometric equations. *Silva Fennica*, 45(3B), 477-569.

Huete, A.R. 1988. A Soil-Adjusted Vegetation Index (SAVI). *Remote Sensing of Environment*,25,295-309.

INPE, 2014. Projeto Prodes - Monitoramento Da Floresta Amazônica Brasileira Por Satélite, INPE, São José dos Campos, Brazil. http://www.obt.inpe.br/prodes/index.php

IPCC, 2003. Definitions and methodological options to inventory emissions from direct human-induced degradation forest and vegetation of other vegetation types. Ninth session of the Conference of the Parties (COP 9). Retrieved on 7th January 2014 from:
http://unfccc.int/meetings/milan_dec_2003/session/6271/php/view/reports.php

IPCC, 2006. IPCC Guidelines for National Greenhouse Gas Inventories. Prepared by the National Greenhouse Gas Inventories Programme. Eds. Eggleston H. S., Buendia L., Miwa K., Ngara T. and Tanabe K. Institute For Global Environmental Strategies, Japan.

Isango, J.A. 2007. Stand structure and tree species composition of Tanzania Miombo Woodlands: a case study from Miombo Woodlands of community based forest management in Iringa District. *Working Papers of the Finnish Forest Research Institute*, 50, 43–56.

Kashaigili, J., Mdemu M., Nduganda A. et al. 2013. Integrated Assessment of Forest Cover Change and Above-Ground Carbon Stock in Pugu and Kazimzumbwi Forest Reserves, Tanzania. *Advances in Remote Sensing*, 2(1), 1-9. doi: 10.4236/ars.2013.21001.

Laser Technology Inc., 2011. TruPulse® 360°R User Manual. www.lasertech.com

Lewis, S., Sonke B., Sunderland T. *et al*. 2013. Aboveground biomass and structure of 260 African tropical forests. *Philosophical Transactions of the Royal Society B.* 368, 20120295.
http://dx.doi.org/10.1098/rstb.2012.0295

Lowe, A.J., Clarke G.P., 2000. Vegetation Structure. In Burgess N.D. & Clarke G.P. (Eds.) 2000. Coastal Forest of Eastern Africa. IUCN, Gland, Switzerland and Cambridge, UK, (Chapter 3.3).

Lu, D. 2005. Aboveground biomass estimation using Landsat TM data in the Brazilian Amazon. *International Journal of Remote Sensing*, 26, 2509-2525.

Luoga, E.L., Witkowski E.T.F., Balkwill, K. 2002. Harvested and standing wood stocks in protected and communal miombo wodlands of eastern Tanzania. *Forest Ecology and Management,* 164, 15-30.

Magnussen, S., Reed, D. *et al.* 2004. Modelling for Estimation and Monitoring. Chapter in *National Forest Assessment Knowledge Reference*. FAO, Rome, Italy.
Retrieved from http://www.fao.org/forestry/8758/en/, on 19th June 2014.

Mdemu, M., Kashaigili, J.J, Lupala, J. *et al.* 2012. Dynamics of land use and land cover changes in the Pugu and Kazimzumbwi forest reserves. *Proceedings of the first Climate Change Impacts, Mitigation and Adaptation Programme Scientific Conference. Dar Es Salaam, Tanzania, 2nd and 3rd January, 2012.* The Climate Change Impact Adaptation and Mitigation (CCIAM) Programme, Sokoine University of Agriculture, Morogoro, Tanzania , 54-76.

Mwampamba, H. 2007. Has the woodfuel crisis returned? Urban charcoal consumption in Tanzania and its implications to present and future forest availability. *Energy Policy* 35(8), 4221-4234.

NAFORMA, 2010a. Field Manual, Biophysical survey. Ministry of Natural Resources and Tourism, Forestry and Beekeeping Division, Dar es Salaam, Tanzania.

NAFORMA, 2010b. Species List sorted by vernacular names (common names). Ministry of Natural Resources and Tourism, Forestry and Beekeeping Division, Dar es Salaam, Tanzania.

O'Brien, S.T., Hubbell, S.P., Spiro, P. *et al*. 1995. Diameter, height, crown, and age relationship in eight neotropical tree species. *Ecology*, 76(6), 1926-1939 Article DOI: 10.2307/1940724

R Core Team, 2012. R: A language and environment for statistical computing. R Foundation for Statistical Computing, Vienna, Austria. ISBN 3-900051-07-0, http://www.R-project.org/.

Sarker, L.R. & Nichol, J.E 2011. Improved forest biomass estimates using ALOS AVNIR-2 texture indices. *Remote Sensing of Environme*nt, 115, 968-977.

Solano, R., Didan K., Jacobson A. *et al.* 2010. MODIS Vegetation Index User's Guide (MOD13 Series). Version 2.00, May 2010 (Collection 5). Vegetation Index and Phenology Lab. University of Arizona.

Tomppo, E., Katila, M., Mäkisara, K., *et al.* 2010. A Report to the Food and Agriculture Organization of the United Nations (FAO) in support of Sampling Study for National Forestry Resources Monitoring and Assessment (NAFORMA) in Tanzania. Retrieved on 28th August 2014 from:
http://www.fao.org/forestry/17847/en/tza/

Trimble, 2011. eCognition® Developer 8.7 Reference Book.

Trimble, 2014. Datasheet: Juno SB handheld. Accessed on 1st August 2014:
http://49.128.56.163/hydronav/templates/rhuk_milkyway/gg/pdf/Juno%20SB.pdf.

White, F. 1983. Vegetation map of Africa. UNESCO/AETFAT /UNSO, Paris, France.

UNFCCC, 2001. The Marrakesh Accords. Seventh session of the Conference of the Parties (COP 7). Retrieved on 7th January 2014 from:

http://unfccc.int/meetings/marrakech_oct_2001/session/6273/php/view/reports.php

UNFCCC, 2009. Fifteenth session of the Conference of the Parties (COP 15). Retrieved on 9th January 2014 from: http://unfccc.int/meetings/copenhagen_dec_2009/session/6262.php

UNFCCC, 2011. Report of the Conference of the Parties on its sixteenth session, held in Cancun from 29 November to 10 December 2010: Retrieved on 19th November 2014 from: http://unfccc.int/resource/docs/2010/cop16/eng/07a01.pdf

UN-REDD, 2009. Tanzania final UN-REDD National Joint Programme. Retrieved on 7th January 2014 from: http://www.unredd.org/UNREDDProgramme/CountryActions/Tanzania/tabid/1028/language/en-US/Default.aspx

UN-REDD, 2012a. Draft Action Plan for implementation of National Strategy for REDD+. Retrieved on 7th January 2014 from: http://www.unredd.org/UNREDDProgramme/CountryActions/Tanzania/tabid/1028/language/en-US/Default.aspx

UN-REDD, 2012b. National Strategy for Reducing Emissions from Deforestation and Forest Degradation (REDD+). Retrieved on 7th January 2014 from: http://www.unredd.org/UNREDDProgramme/CountryActions/Tanzania/tabid/1028/language/en-US/Default.aspx

UN-REDD, 2013. Roadmap for Development of a Reference Emission Level / Reference Level for the United Republic of Tanzania. Discussion draft – v1.

Note: The links to UN-REDD are no longer active

## 8.1 Remote Sensing and GIS data:

Quickbird, Worldview-2, IKONOS and Geoeye-1 satellite data, from Digital Globe:
https://browse.digitalglobe.com/

Rapideye satellite data, from Eyefind:
http://eyefind.rapideye.de/

Landsat, from USGS:
http://earthexplorer.usgs.gov/

Climatic diagram from Cisgrasp:
http://cigrasp.pik-potsdam.de/diagrams/compare

Global ecological zones of the World, FAO 2001:
http://www.fao.org/geonetwork/srv/en/main.home

White’s vegetation map of Africa, from UNESCO/AETFAT/UNSO 1983 (provider UNEP):
http://ede.grid.unep.ch/

Climatic zones from FAO forestry country information (2012):
http://www.fao.org/forestry/country/18310/en/tza/

Hunting's vegetation map 1996: courtesy of TFS.

## 8.2 Software

*COPIKS PhotoMapper*, from COPIKS:
http://software.copiks.com/photomapper

*DNR Garmin application (*DNRGPS), from Minnesota Department of Natural Resources:
http://www.dnr.state.mn.us/mis/gis/tools/arcview/extensions/DNRGarmin/DNRGarmin.html

*MapSmart Field Mapping Software*, from Laser Inc Technology:
http://www.lasertech.com/MapSmart-Software.aspx

# Annex I. Field support documents

## Field forms

Annex table 1: Waypoint form.

| WAYPOINT | | | |
|---|---|---|---|
| ID Number | GPS coordinates | Photo ID | Notes |
| | | | |
| | | | |

Annex table 2: Plot form.

| PLOT | | | | | | | | | | | |
|---|---|---|---|---|---|---|---|---|---|---|---|
| Plot number | field site | | | | | | | | | | |
| Forest | area name | | | | | | | | | | |
| Date and time | | | | | | | | | | | |
| Centre GPS coordinates | | X | | | | Y | | | | | |
| UTM zone | | | | | | | | | | | |
| Slope (%) | | | | | | | | | | | |
| Photo ID in camera | | C | | N | | E | | S | | W | |
| Canopy cover | | C | | N | | E | | S | | W | |
| Vegetation type | | *(table A5)* | | | | | | | | | |
| Undergrowth type | % cover | *(table A6)* | | | | | | | | | |
| Damage - severity | | *(table A7)* | | | | | | | | | |
| Human impact | estimated time | *(table A8)* | 1 | | | | | | | | |
| | | | 2 | | | | | | | | |
| | | | 3 | | | | | | | | |
| Land use | | *(table A9)* | | | | | | | | | |
| *Notes* | | | | | | | | | | | |

Annex table 3: Tree form.

| TREES | | | | | | | | | | |
|---|---|---|---|---|---|---|---|---|---|---|
| Plot no. | Tree no. | Specie (vernacular and botanic names) | Distance to centre (m) | Azimuth (°) | Crown diameter (m) | Total height (m) | Stem no. | DBH (cm) | Tree utilities | Notes (health…) |
| | | | | | | | | | | |
| | | | | | | | | | | |

Note: When a tree has several stems, plot and tree number, specie distance to centre, azimuth and crown diameter are recorded only once.

Annex table 4: Stump form.

| STUMP FORM | | | | | |
|---|---|---|---|---|---|
| Stump no. | Specie | Diameter below cutting point or DBH | Height | Estimated years from cutting | Remarks |
| | | | | | |
| | | | | | |
| | | | | | |

## Field codes

Annex table 5: Vegetation codes. A full vegetation code is composed by a sequential concatenation of the codes in the table from the different levels (*E.g.* B_L_O_Et: Bushland low and open with emergent trees).

| **Vegetation codes** | | | | | | | |
|---|---|---|---|---|---|---|---|
| **Level 1** | | **Level 2** | | **Level 3** | | **Level 4** | |
| **F** | Forest | **C** | closed (>90%) | **hm** | humid mountain | | |
| | | **O** | open (<90%) | **l** | lowland | | |
| | | | | **m** | mangrove | | |
| **W** | Woodland | **C** | closed (<40%) | | | | |
| | | **O** | open (>40%) | | | | |
| **B** | Bush | **H** | high (>2m) | **d** | dense | +Et | emergent trees |
| | | **S** | low (>2m) | **o** | open | | |

Annex table 6: Undergrowth codes.

| **Undergrowth codes** | |
|---|---|
| **0** | No vegetation |
| **1** | Bushes |
| **2** | Elephant grass |
| **3** | Grass |
| **4** | Herbs |
| **5** | New tree generation |
| **6** | Other vegetation (specify) |

Annex table 7: Damage codes.

| **Damage codes** | |
|---|---|
| **0** | No damage |
| **1** | Fire |
| **2** | Biotic factors (insects, fungus, disease, other) |
| **3** | Abiotic factors (wind, other) |
| **4** | Human activities |

Annex table 8: Human impact codes.

| **Human impact codes** | |
|---|---|
| **0** | No human impact |
| **1** | Selective cutting (commercial use) |
| **2** | Selective cutting (domestic use) |
| **3** | Clear felling |
| **4** | Illegal cutting |
| **5** | Timber sawing |
| **6** | Charcoal production |
| **7** | Burning |
| **8** | Afforestation |
| **9** | Agricultural clearance |
| **10** | Other (specify) |

Annex table 9: Land use codes.

| Human impact codes | |
|---|---|
| **0** | Plantation / Production forest |
| **1** | Protection forest |
| **2** | Wildlife reserve |
| **3** | Shifting cultivation |
| **4** | Agriculture |
| **5** | Grazing land |
| **6** | Other (specify) |

## Radius correction table

Annex table 10: Radius correction table according to slope.

| Slope (%) | Radius (m) |
|---|---|
| **5** | 10.02 |
| **10** | 10.06 |
| **15** | 10.14 |
| **20** | 10.25 |
| **25** | 10.40 |
| **30** | 10.59 |
| **35** | 10.83 |
| **40** | 11.12 |
| **45** | 11.47 |
| **50** | 11.89 |
| **55** | 12.41 |
| **60** | 13.04 |
| **65** | 13.83 |
| **70** | 14.84 |
| **75** | 16.17 |
| **80** | 17.99 |

## Laser rangefinder routine measurement for slope and position

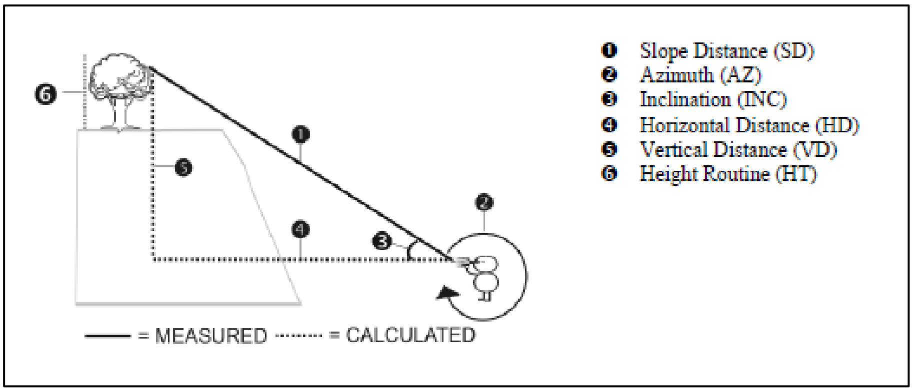


$$\tan 3 = \frac{5}{4}$$

Annex figure 1: Laser rangefinder routine to measure slope, distance and azimuth (source: Laser Technology Inc. 2011) and geometry.

## Annex II. Statistical analysis

### Correlation matrix among parameters

The following matrixes represent the correlation results between the remote sensing parameters: GLCM texture features (Angular 2nd moment, Contrast, Dissimilarity, Entropy, Homogeneity in all directions, Homogeneity at 45°, Mean and Variance), the mean band reflectance (of band 1, 2, 3 and 4), the standard deviation ratio of bands 3 and 4, the standard deviation band reflectance (of 1, 2, 3 and 4) and the vegetation index NDVI, with the field parameters: basal area (BA), DBH, volume, height and biomass. The parameters are represented in this order in the matrix diagonal. On the top triangle, the sizes of the circles represent the value (from 0 to 1) s and the colour the sign (+/-) of the correlation coefficient. On the bottom triangle, there are the values of the correlation coefficients. The crosses indicate the no significant correlations (p-value = 0.05).

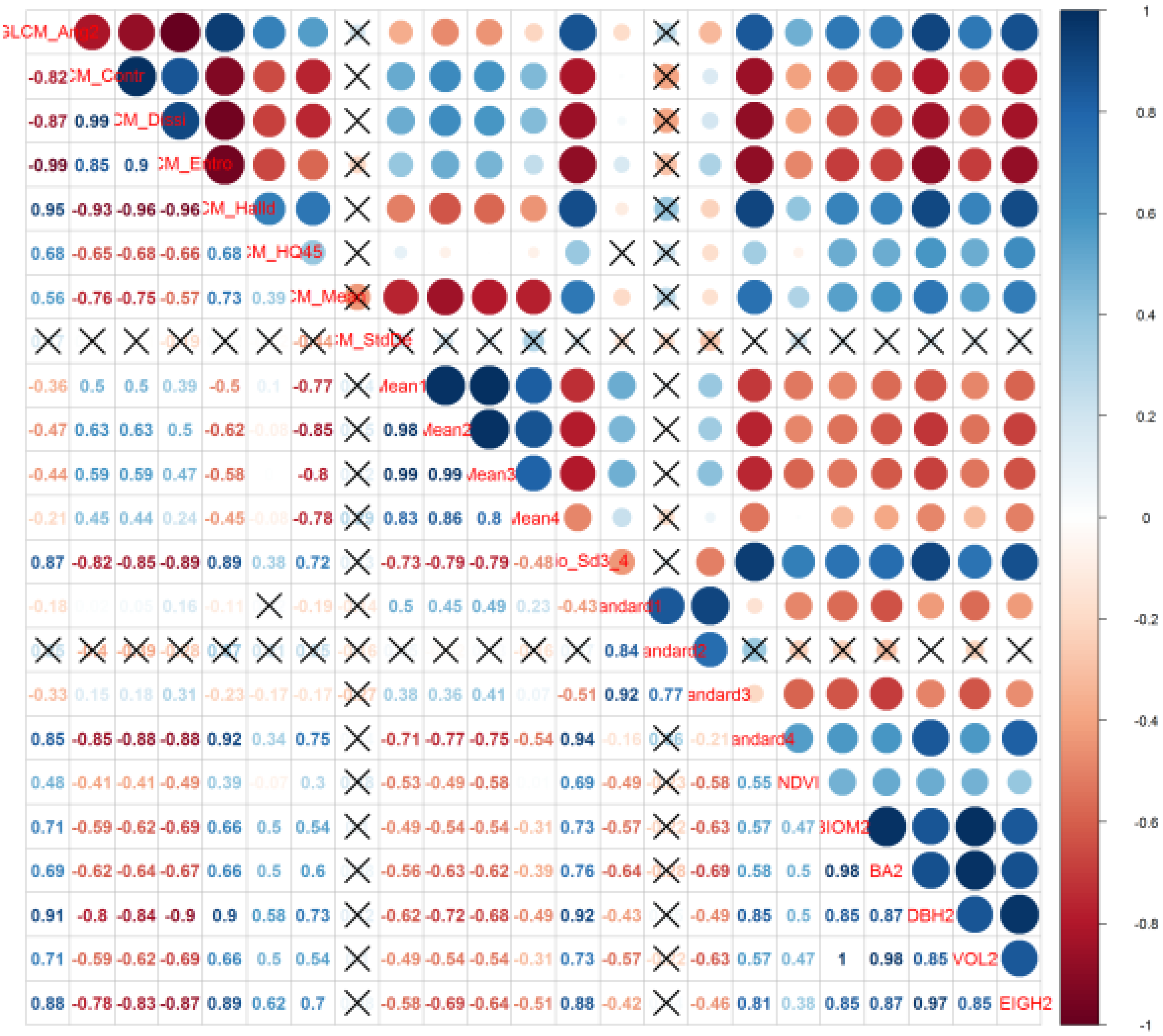

Annex figure 2: Correlation matrix among remote sensing and field parameters (biomass, basal area, DBH, volume, height).

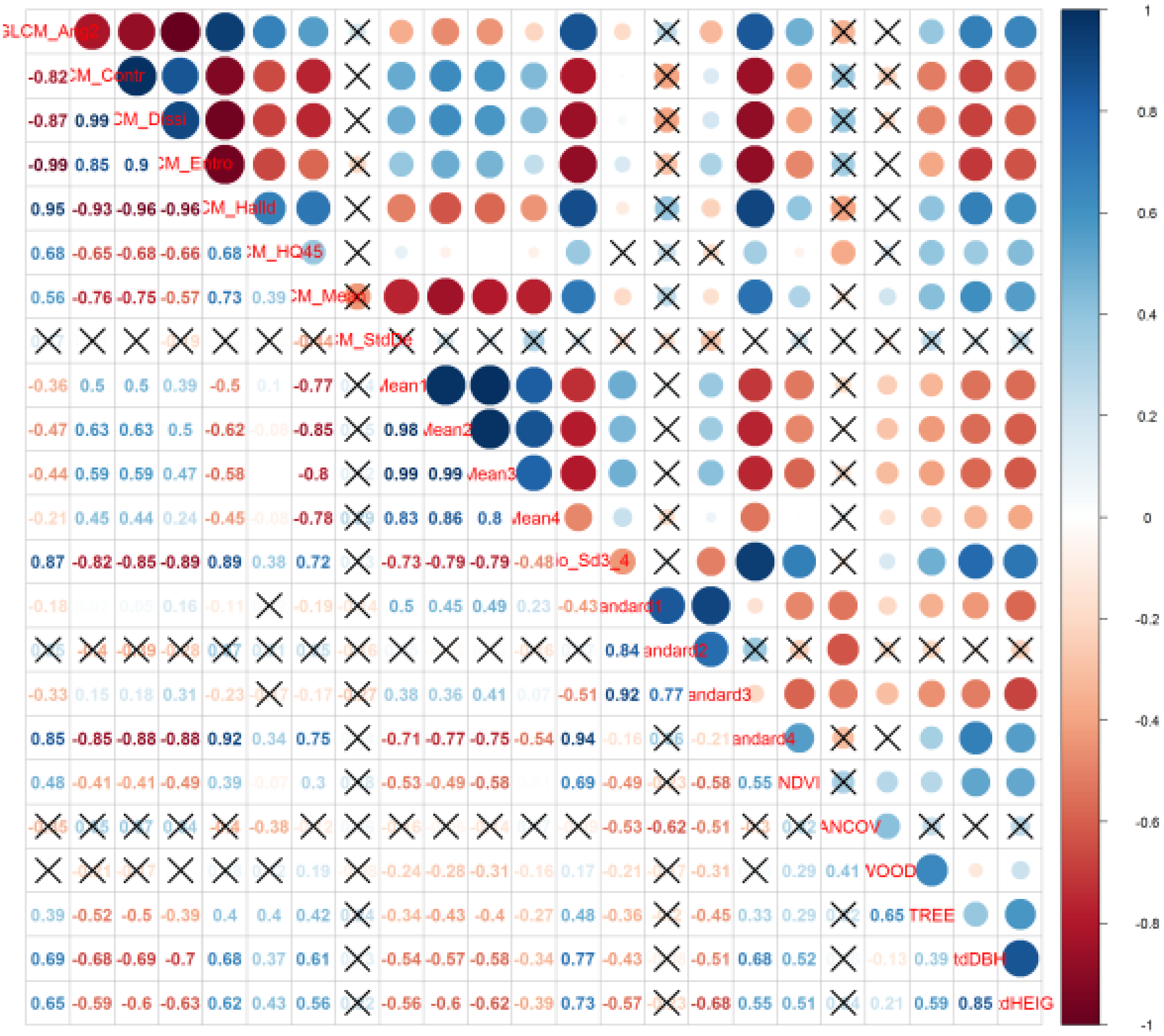

Annex figure 3: Correlation matrix among remote sensing and field parameters (canopy cover, wood species, tree species, standard deviation of DBH and standard deviation of height).

## Correlation matrix among the independent remote sensing parameters

This matrix leaves the explanatory variables with a correlation of less than 0.70.

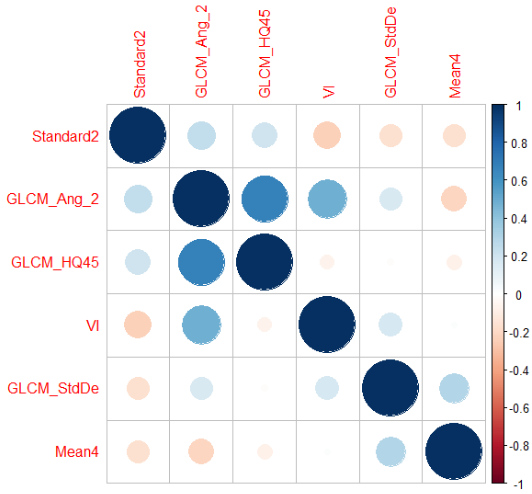


Annex figure 4: Correlation matrix among the independent remote sensing parameters (correlation of less than 0.70).

## Scatter plots for the multiple regression models

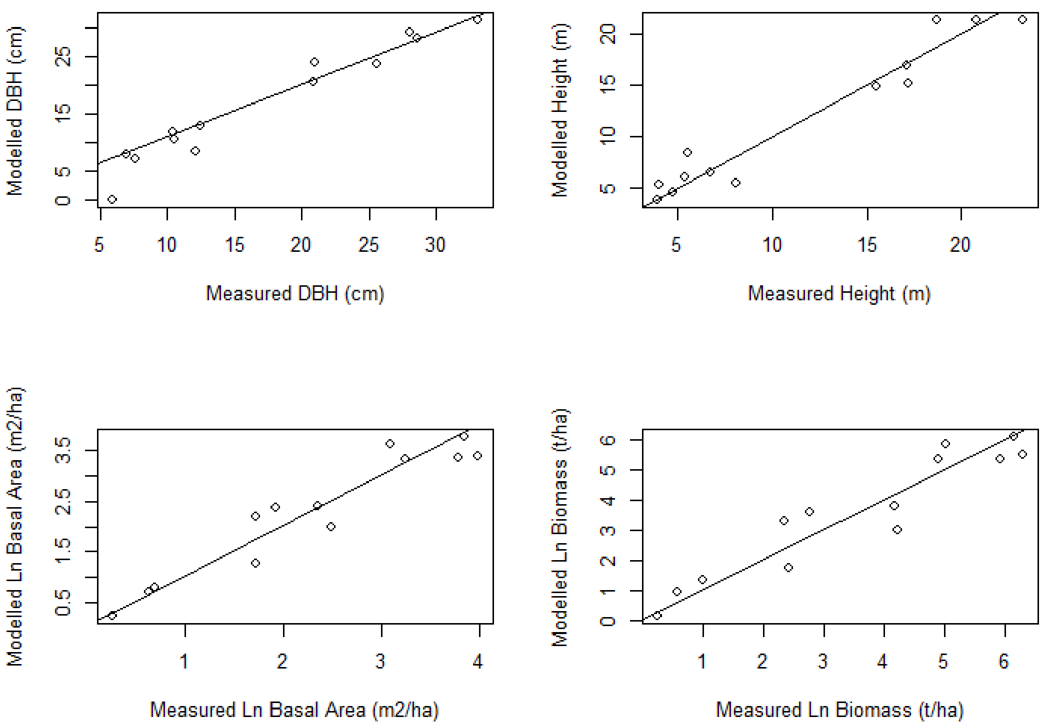


Annex figure 5: Scatter plots and linear regression line between the field measured data and the modelled results for DBH, height, basal area and biomass.

**Relationship between tree height and estimated canopy cover for validation**

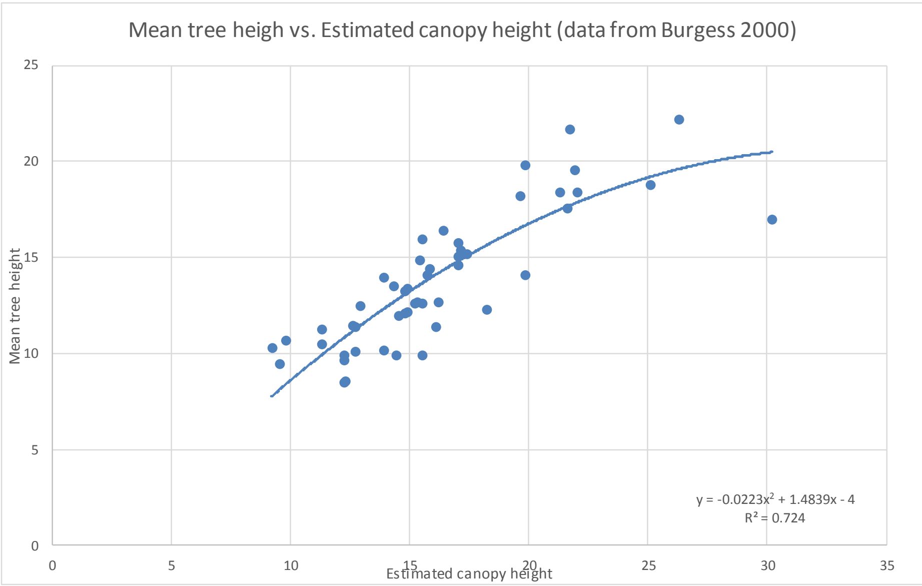


Annex figure 6: Plot of mean tree height vs. estimated canopy cover from Burgess 2000.

European Commission
EUR 26922 – Joint Research Centre – Institute for Environment and Sustainability

Title: Field guide for forest mapping with high resolution satellite data

Author(s): Lorena Hojas Gascón, Hugh Eva

Luxembourg: Publications Office of the European Union

2014 – 75 pp. – 21.0 x 29.7 cm

EUR – Scientific and Technical Research series – ISSN 1831-9424 (online)

ISBN 978-92-79-44012-0 (PDF)

doi:10.2788/657954

Abstract

This manual is targeted at guiding the collection of adequate field information in a relatively short time, for calibrating and validating classifications and biophysical parameters derived from satellite images of high spatial resolution for forest monitoring. It aims to support of monitoring deforestation and forest degradation in the context of the UN-REDD (Reducing Emissions from Deforestation and Degradation) programme.

Experience gained from field surveys carried out in conjunction with the Tanzania Forest Service in 2012, 2013 and 2014 in the Pugu Hills Forest Reserve is used to demonstrate the methods of data collection and analysis. The field data collected in this work were used to produce maps of forest cover, basal area and biomass. These maps were transferred to the Tanzania Forest Service to support their forest inventory

LB-NA-26922-EN-N

## JRC Mission

As the Commission's in-house science service, the Joint Research Centre's mission is to provide EU policies with independent, evidence-based scientific and technical support throughout the whole policy cycle.

Working in close cooperation with policy Directorates-General, the JRC addresses key societal challenges while stimulating innovation through developing new methods, tools and standards, and sharing its know-how with the Member States, the scientific community and international partners.

*Serving society*
*Stimulating innovation*
*Supporting legislation*

Publications Office

ISBN 978-92-79-44012-0